Pure Appl. Geophys.
© 2026 The Author(s), modified publication 2026
https://doi.org/10.1007/s00024-026-04007-x

Pure and Applied Geophysics

Evaluation of the Consistency Between SPI, PNI, and DDI Drought Indices in the Asi Basin

Mehmet Can Topboğazı,[1] Seda Sever,[1] and Recep Yurtal[1]

Abstract—This study evaluates the consistency between three precipitation-based drought indices—the Standardized Precipitation Index (SPI), Percent of Normal Index (PNI), and Deciles Drought Index (DDI)—in the Asi Basin, Türkiye. Using 32–52 years of precipitation data from 11 stations, drought conditions were analyzed at monthly, seasonal, and annual scales. To ensure statistical robustness, Mann–Kendall trend tests were applied, and Bartlett-corrected effective sample sizes were used to account for temporal autocorrelation in correlation analyses. Additionally, a sensitivity analysis using a common 30th percentile threshold was conducted to evaluate the influence of classification schemes. The results reveal strong agreement between DDI and PNI, while consistency with SPI decreases during dry summer months (July–August) due to the mathematical instability of PNI under zero-dominated rainfall regimes. Trend analysis identified a statistically significant drying trend at the Hassa station ($p < 0.05$) across all indices, despite no basin-wide trend being detected. The use of 95% confidence intervals highlighted increased uncertainty at longer temporal scales due to autocorrelation. For operational purposes, it is recommended to interpret PNI with caution during hyper-arid periods and to use SPI as a proxy for potential hydrological drought. Overall, the findings emphasize the necessity of multi-index frameworks that account for both climatic variability and methodological constraints.

Keywords: Drought monitoring, standardized precipitation index (SPI), deciles drought index (DDI), percent of normal index (PNI), Mediterranean climate, correlation analysis, Asi Basin.

Abbreviations

SPI	Standardized precipitation index
DDI	Deciles drought index
PNI	Percent of normal index
PDSI	Palmer drought severity index
Jan	January
Feb	February
Mar	March
Apr	April
May	May
Jun	June
Jul	July
Aug	August
Sep	September
Oct	October
Nov	November
Dec	December
JJA	June–July–August

1. Introduction

Drought is a natural phenomenon that adversely affects the sustainable management of water resources, agricultural productivity, and socio-economic systems, typically arising when precipitation falls substantially below long-term climatological norms. It is widespread throughout the world, particularly in arid and semi-arid regions. While definitions of drought vary across disciplines, there is no universally accepted definition. Generally, it is described as a temporary reduction in streamflow and soil moisture, initiated by a prolonged precipitation deficit (Şen, 2015; Wilhite & Glantz, 1985). Drought is a natural part of the climate and is affected by climate change (WMO, 2022). The IPCC (2021) report highlights that climate change has intensified the frequency and magnitude of droughts in many regions worldwide. Furthermore, the IPCC (2023) projections indicate a high likelihood of concurrent drought occurrences across multiple regions, implying that both the risk and frequency of drought events are expected to increase globally. As such, the risk and frequency of drought events are projected to increase in many regions. Droughts rank among the most economically damaging natural hazards, with

[1] Civil Engineering Department, Engineering Faculty, Çukurova University, Adana, Türkiye. E-mail: mtopbogazi@gmail.com; ssever@cu.edu.tr; ryurtal@cu.edu.tr

Published online: 19 June 2026

the capacity to simultaneously affect multiple economic sectors and large populations. Without adequate planning and preparedness, the impacts of drought on agriculture, water resources, and natural ecosystems can worsen or lead to severe consequences (Jain et al., 2015; Yihdego et al., 2019).

Wilhite and Glantz (1985) categorized drought into four classes: meteorological, agricultural, hydrological and socioeconomic drought, respectively. Meteorological drought is the initial type of drought, characterized by precipitation levels falling below the normal range. Agricultural drought occurs when there is insufficient water to meet the irrigation needs of crops during critical periods of the growing season (Heim, 2002; Wilhite & Glantz, 1985). Hydrological drought refers to a decline in water resources due to prolonged precipitation deficits (Heim, 2002; Mishra & Singh, 2010; Wilhite & Glantz, 1985). Socioeconomic drought links the supply and demand of certain economic goods to meteorological, agricultural, and hydrological drought conditions, negatively affecting societal well-being (Öz et al., 2024; Wilhite & Glantz, 1985). Unlike other natural disasters such as floods, droughts are typically not confined to small areas nor do they occur within clearly defined time intervals; therefore, they are difficult to delineate both spatially and temporally (Nikbakht et al., 2013; Vicente-Serrano et al., 2011). Severe and extreme droughts generally manifest over extensive spatial domains, in contrast to mild and moderate droughts that predominantly occur within more localized areas (Degefu & Bewket, 2015). Drought has different regional characteristics as it is influenced by climatological and hydrological parameters (Topçu et al., 2022). Understanding a drought event depends on information about the area, severity and duration of the drought. Drought indices have been developed to assess the impact of drought and to determine different drought parameters such as intensity, duration and spatial distribution (Hao et al., 2016; Heim, 2002; Keyantash & Dracup, 2002; Li et al., 2024; Öz et al., 2024; Vicente-Serrano et al., 2010). Drought characteristics are commonly analyzed using various indices, among which the Palmer Drought Severity Index (PDSI), developed by Palmer (1965), is one of the most widely used. This index integrates variables such as average monthly or weekly temperature, total precipitation, soil moisture, and potential evapotranspiration (Serkendiz et al., 2024). The Standardized Precipitation Index (SPI), developed by McKee et al. (1993), is one of the most widely used drought indices in the literature due to its ability to be calculated only based on precipitation data, its applicability for comparisons across different climate regions, and its effectiveness in identifying dry periods (WMO, 2012). The Standardized Precipitation Evapotranspiration Index (SPEI), developed by Vicente-Serrano et al. (2010) is a multiscalar drought index that incorporates both precipitation and evapotranspiration data. It stands out not only for its ability to identify drought across different temporal scales but also for integrating both precipitation and temperature variables (Tirivarombo et al., 2018). In addition to the widely used drought indices in the literature, various other indices have been developed to capture the complex and multifaceted nature of drought. The Deciles Drought Index (DDI) developed by Gibbs and Maher (1967), where long-term precipitation data are divided into deciles, is one of the original methods used in drought analysis. In this method, long-term precipitation records are divided into deciles, and the severity of drought is determined based on the decile class to which the observed precipitation values fall at daily, weekly, monthly, or annual time scales (Dikici & Aksel, 2021; WMO, 2016). The Percent of Normal Index, which can be calculated for daily, weekly, monthly, seasonal and annual time intervals, is one of the drought indices used (WMO, 2016).

The Standardized Precipitation Index (SPI) is among the most widely applied indicators for drought assessment. It relies solely on precipitation data to quantify the extent to which rainfall during a given period deviates from long-term climatic norms, making it an effective tool for identifying drought conditions across multiple temporal scales (Yüceer & Aktürk, 2025). Globally, the SPI has been extensively evaluated and compared with other drought indices (Arra & Sisman, 2024; Labudová et al., 2017; Shokoohi & Morovati, 2015; Soláková et al., 2014; Wable et al., 2018; Zeybekoğlu & Aktürk, 2021; Zhai et al., 2010) Several comparative studies have evaluated the performance of different drought indices to assess their consistency and applicability across

diverse climatic and temporal conditions. For instance, Wu et al. (2001) compared the SPI, the China-Z Index, and the Statistical Z-score in several regions of China and demonstrated that these indices produced comparable results, with the latter two being computationally simpler. Similarly, Dogan et al. (2012) analyzed six indices, including SPI and PNI, in Konya, Türkiye, and reported that the SPI yielded more consistent results across multiple time scales. Moreover, Morid et al. (2006) evaluated seven drought indices, including SPI, DDI, and PNI, in Tehran Province, Iran, and found that the SPI effectively identified the onset of drought and captured its spatial and temporal variability, underscoring its suitability for operational drought monitoring. In a similar context, Nohegar et al. (2015) examined drought patterns in the Hormozgan region of Iran and concluded that PNI, DDI, and SPI were the most suitable indices for determining drought frequency and severity. Likewise, Salehnia et al. (2017) investigated historical drought events in the Kashafrud Basin of Iran using eight indices, including SPI, PNI, and DDI, and observed a strong correlation among them ($R^2 = 0.99$), confirming their high degree of consistency in drought characterization. Recently, Yüceer and Aktürk (2025) conducted a comprehensive investigation of the spatio-temporal characteristics of meteorological droughts in the Kızılırmak Basin, employing two distinct drought indices RDI (Reconnaissance Drought Index) and SPI, and demonstrated the effectiveness of both indices in regional drought assessment.

The Asi Basin holds strategic importance for Türkiye due to its location in the southern part of the country and its rich hydrological and agricultural potential under the influence of the Mediterranean climate. The basin stands out particularly in the production of cotton, olives, citrus, and various vegetables. This intensive agricultural activity exerts significant pressure on water resources. The high demand for irrigation makes the efficient use and sustainable management of water at the basin scale indispensable. In addition, the transboundary nature of the Asi River renders the basin critical not only at the national but also at the regional level. Therefore, the sustainable management of water resources has become increasingly important for agricultural production, domestic water supply, and ecosystem services. However, due to the high variability of seasonal and annual precipitation, the basin is highly vulnerable to drought. Drought, in particular, has become more pronounced during the spring season (Çelik, 2019). This situation threatens the continuity of agricultural production and increases uncertainties in the planning and management of water resources. Hence, regular monitoring of drought and its evaluation through different drought indices are of great importance for ensuring regional food security and achieving sustainable water resources management. Drought has transboundary impacts and is a critical issue for planning, risk management, and sustainable water policies. In this context, monitoring and assessing drought is particularly important in the Asi Basin, a strategic transboundary water resource.

Drought analyses have been conducted across Türkiye on monthly, seasonal, and agricultural year scales using the Standardized Precipitation Index (SPI) and the Percent of Normal Index (PNI) (Şimşek, 2010). The 2007–2008 drought in Türkiye was analyzed using the Standardized Precipitation Index (SPI), the Percent of Normal Index (PNI), as well as temperature and precipitation data (Şimsek & Çakmak, 2010). Meteorological and hydrological droughts were analyzed over a broad area using data from 48 meteorological and 55 streamflow observation stations across Türkiye, highlighting the occurrence of drought events particularly in the Mediterranean Region of the country (Özfidaner, 2020). Gümüş (2017) investigated hydrological drought in the Asi River Basin using the Streamflow Drought Index (SDI) at 3-, 6-, and 12-month time scales, and identified the year 2000 as the period of the most severe drought. In the study, the proportions of extreme, severe, and moderate droughts across the stations were calculated as 3%, 5%, and 10%, respectively. Dikici (2019) stated that there is a slow drought trend in the Asi Basin. Topboğazı et al. (2022) reported that the most frequent drought in the Asi Basin was observed in the spring season. Turhan et al. (2022) evaluated the drought in Arsuz Plain in the Asi Basin in terms of hydrological aspects and stated that the frequency of drought increased. Dikici (2020) conducted a drought risk analysis in the Asi Basin with the help of different drought indices

including SPI to estimate the magnitude and severity of droughts. Topçu and Seçkin (2022) stated that the frequency and severity of drought increased in the Asi Basin after the 1990s.

In this study, a comprehensive drought assessment was conducted for the Asi Basin in southern Türkiye, a region characterized by a Mediterranean climate with distinct wet and dry seasons. Three precipitation-based drought indices—the Standardized Precipitation Index (SPI), Deciles Drought Index (DDI), and Percent of Normal Index (PNI)—were employed to investigate the spatio-temporal variability of meteorological droughts across the basin. Long-term precipitation records spanning 32–52 years from 11 meteorological stations were analyzed at monthly, seasonal, and annual scales. To ensure statistical robustness, the methodology was enhanced by incorporating non-parametric Mann–Kendall tests to evaluate temporal trends and Bartlett-type corrections to account for temporal autocorrelation in correlation analyses. In addition, a sensitivity analysis based on a common 30th percentile threshold was introduced to rigorously assess the influence of index-specific classification schemes on inter-index consistency. By integrating multiple indices, temporal resolutions, and uncertainty quantification through 95% confidence intervals, the study provides a comprehensive and methodologically robust understanding of regional drought behavior and inter-index relationships. The results contribute to improving drought monitoring capacity in southern Türkiye and provide practical guidance for sustainable water resource management and climate-resilient strategies in the Asi Basin. Given the transboundary nature of the Asi Basin, shared by Türkiye, Syria, and Lebanon, understanding its spatio-temporal drought dynamics and long-term trends is essential not only for improving drought preparedness but also for supporting cooperative transboundary water governance. This study fills an important gap in the literature by providing a multi-temporal assessment that explicitly accounts for both methodological constraints and statistical uncertainties in the Asi Basin under Mediterranean climatic conditions.

2. Methodology and Data

2.1. Research Area and Data

The Asi Basin is located in the Eastern Mediterranean Region, between 36° 21′ north and 35° 48′ south latitudes, 36° 41′ east and 35° 53′ west longitudes. It has a drainage area of 7886.3 km^2 within the borders of Türkiye. The Asi basin is bordered by the Mediterranean Sea to the west, Syria to the south, the

Table 1

Information on meteorological stations

Station Name	Station no.	Observation Years	Observation Period (year)	Latitude	Longitude	Elevation (m)
Antakya	17372	1970–2021	52	36.2	36.1	158
Dörtyol	17962	1970–2021	52	36.8	36.2	27
İskenderun	17370	1970–2021	52	36.6	36.2	2
İslahiye	17964	1970–2021	52	37.0	36.6	470
Samandağ	17986	1970–2021	52	36.1	35.9	6
Altınözü	18058	1987–2021	35	36.1	36.2	341
Arsuz-Uluçınar	18858	1970–2001	32	36.4	35.9	24
Belen	18057	1988–2021	34	36.5	36.2	624
Hassa	18275	1977–2021	45	36.8	36.5	377
Kırıkhan	18276	1970–2021	52	36.5	36.3	218
Yeşilkent-Erzin	18274	1987–2021	35	37.0	36.2	185

Euphrates Basin to the east and the Ceyhan Basin to the north. It has an average annual rainfall of 785.5 mm and an average annual runoff of 2.8 km^3. In the section of the Asi River within the borders of Türkiye, the characteristics of the transitional climate between Central Anatolia and the Mediterranean are observed at the upper elevations, while the typical Mediterranean climate characteristics become more prominent as it descends at lower elevation. Table 1 shows the study area and the locations of the meteorological stations within the Asi Basin that were used in the analysis.

The data used in this study were obtained from the Turkish State Meteorological Service. The study utilized data from eleven meteorological stations, each with a minimum of 32 years of observational records. The locations of the meteorological stations used in this study are shown in Fig. 1.

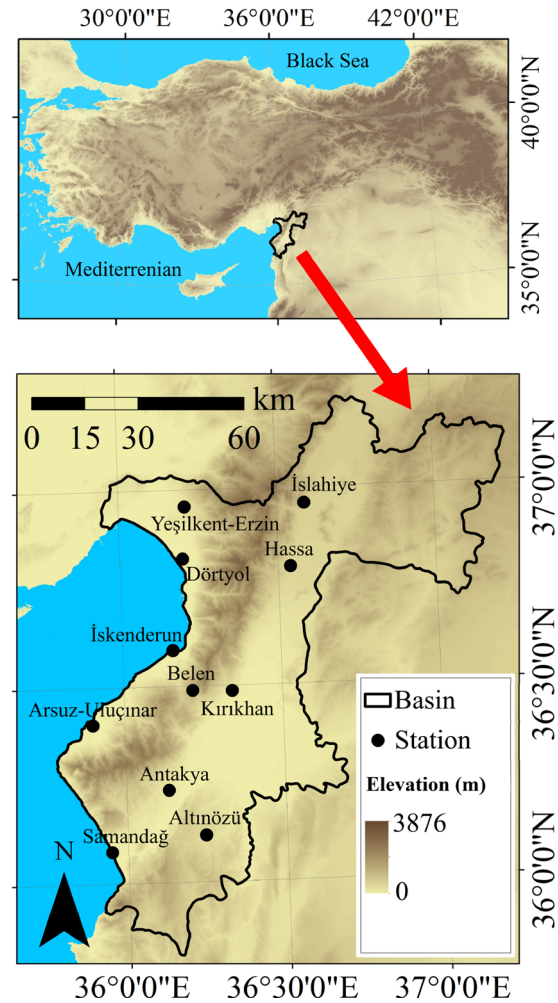


Figure 1
Asi Basin and location of stations in the Asi Basin

2.2. *Missing Data Imputation*

In some stations within the study area, missing data were observed for certain periods. These missing data were addressed using reliable methods, thereby ensuring the integrity of the dataset. In filling the missing data, inter-station statistical similarity was taken as the basis. Accordingly, the missing observations of a station for a given month were completed using data from the neighboring station that exhibited the highest correlation coefficient with the target station. The strong correlation between the stations indicated a reliable linear relationship, thereby providing the basis for regression modeling. The strong correlation between the stations indicated a reliable linear relationship, thereby forming the basis for regression modeling. However, due to minimal or no precipitation during the summer months under the Mediterranean climate, high correlations between stations could not be established for this period. Therefore, the missing data for these months were estimated using the Normal Ratio Method.

2.2.1 *Linear Regression*

Linear regression analysis is used to model the relationship between a dependent variable and one or more independent variables. It can be expressed as shown in Eq. (1).

$$y = b_0 + b_1 * x \tag{1}$$

Here, y represents the precipitation value at the station with missing data, b_0 represents the intercept reflecting the systematic difference between the two stations, b_1 denotes the slope between the target station and the key station; and x refers to the precipitation value at the key station.

For the station whose missing data will be completed using the linear regression method, the key station is selected based on the correlation coefficients between stations. For stations with missing data, the station with the highest correlation

coefficient ($r > 0.7$) and complete data for the target period was selected as the donor station for linear regression. The correlation coefficient is calculated as follows (Eq. 2).

$$r_x = \frac{\sum_{i=1}^{n}(x_i - x_{mean})(y_i - y_{mean})}{\sqrt{\sum_{i=1}^{n}(x_i - x_{mean})^2 \sum_{i=1}^{n}(y_i - y_{mean})^2}} \quad (2)$$

In Eq. (2), r_x represents the correlation coefficient, x_i and y_i are the precipitation values of the meteorological stations measured at the same time, x_{mean} and y_{mean} are the average value of the precipitation data of the meteorological stations.

2.2.2 Normal Ratio Method

For stations that did not provide high correlation coefficients between stations, the normal ratio method was used to complete the missing data.

$$P_x = \frac{N_x}{N}\left(\sum_{i=1}^{n}\frac{P_i}{N_i}\right) \quad (3)$$

Here, P_x is the precipitation at the station with missing data, P_i is precipitation value of the key station, N_x is precipitation value of the station with missing data, N_i is long-term average precipitation of the key station, n is number of key stations.

2.3. Standardized Precipitation Index (SPI)

Developed by McKee et al. (1993), the Standardized Precipitation Index (SPI) is an index calculated based on the probability of precipitation over a specific time period (Yihdego et al., 2019). In this method, precipitation data are converted into a single numerical value, allowing calculations to be performed over both short and long time scales. In studies related to meteorological, agricultural, and hydrological drought, drought time scales of 3, 6, 12, 24, 48, and 72 months have been widely calculated and used for practical purposes (Keskiner et al., 2019). The SPI is based on fitting a probability distribution to the precipitation series for a specified time scale and subsequently transforming the observed precipitation values into standardized Z-scores using the inverse of the normal distribution function. For this reason, precipitation data are typically fitted to the Gamma Distribution (McKee et al., 1993), as Thom (1958) indicated that the Gamma distribution is the most suitable probability model for representing climatological time series. Accordingly, both the probability density function (PDF) and the cumulative distribution function (CDF) of this distribution can be utilized in drought analysis. The probability density function of the Gamma distribution is expressed as shown in Eq. (4).

$$g(x) = \frac{1}{\beta^{\alpha}\Gamma(\alpha)}x^{\alpha-1}e^{x/\beta}; x, \alpha, \beta > 0 \quad (4)$$

Here, x denotes the precipitation amount, α is the shape parameter, β represents the scale parameter, and $\Gamma(\alpha)$ is the gamma function. The gamma function and the parameters α and β are respectively given in Eqs. (5), (6), and (7), while n in Eq. (8) denotes the number of precipitation observations.

$$\Gamma(\alpha) = \int_0^{\infty} y^{\alpha-1}e^{-y}dy \quad (5)$$

$$\alpha = \frac{1}{4A}\left(1 + \sqrt{1 + \frac{4A}{3}}\right) \quad (6)$$

$$\beta = \frac{\overline{x}}{\alpha} \quad (7)$$

$$A = ln(x) - \frac{ln\sum(x)}{n} \quad (8)$$

To obtain the cumulative distribution function from the probability density function, Eq. (9) is used.

$$G(x) = \int_0^{x} g(x)dx = \frac{1}{\beta^{\alpha}\Gamma(\alpha)}\int_0^{x} x^{\alpha-1}e^{\frac{-x}{\beta}}dx \quad (9)$$

Because the gamma function is not defined for $x = 0$ and precipitation records may contain zero values, the cumulative probability distribution can therefore be formulated as shown in Eq. (10) (Lloyd-Hughes & Saunders, 2002)

$$H(x) = q + (1 - q)G(x) \quad (10)$$

In Eq. (10), q is obtained by dividing the number of zero-precipitation records by the total number of observations. The cumulative probability $H(x)$ is transformed into a standard normal distribution,

resulting in a standard normal random variable (Z) with a mean of zero (0) and a standard deviation of one (1). This variable represents the SPI value. According to the approximate formula proposed by Abramowitz and Stegun (1965), the standardized normal random variable Z (SPI) is defined as follows (Eqs. 11–14).

$$SPI = -\left(t - \frac{c_0 + c_1 t + c_2 t^2}{1 + d_1 t + d_2 t^2 + d_3 t^3}\right); \quad 0 \qquad (11)$$

$$t = \sqrt{ln\left(\frac{1}{(H(x))^2}\right)}; \quad 0 < H(x) \leq 0.5 \qquad (12)$$

$$SPI = \left(t - \frac{c_0 + c_1 t + c_2 t^2}{1 + d_1 t + d_2 t + d_3 t}\right); \quad 0.5 < H(x) \leq 1 \qquad (13)$$

$$t = \sqrt{ln\left(\frac{1}{(1 - H(x))^2}\right)}; \quad 0.5 < H(x) \leq 1 \qquad (14)$$

Here $c_0 = 2.515517$, $c_1 = 0.802853$, $c_2 = 0.010328$, $d_1 = 1.432788$, $d_2 = 0.189269$, $d_3 = 0.001308$.

In drought analyses based on the Standardized Precipitation Index (SPI) values calculated using the parameters of this distribution, periods when the index is negative are defined as "dry periods". The drought period starts when the index falls below zero and ends when it reaches positive values again. According to this method, the severity levels of drought periods are determined based on the classification in Table 2.

To ensure the robustness of the analysis, the suitability of monthly precipitation data for the Gamma probability density function was rigorously evaluated using both the Kolmogorov–Smirnov (K–S) and Anderson–Darling (A–D) goodness-of-fit tests. While the K–S test assesses the overall agreement between the empirical and theoretical distributions, the A–D test places greater emphasis on deviations in the distribution tails, which is particularly important for drought analyses that are sensitive to extreme low-precipitation events. The tests applied to the 1970–2021 monthly precipitation records yielded highly consistent results across both methods. Approximately 98% of the stations exhibited a statistically significant fit to the Gamma distribution (Table 3), indicating that this model adequately captures the precipitation variability across the basin. Only minor marginal departures were observed at the Hassa and Kırıkhan stations, and these deviations were restricted to the dry months of September (Hassa) and July (Kırıkhan). Despite these marginal deviations, the Gamma distribution was retained for the Hassa and Kırıkhan stations in order to preserve spatial consistency across the basin. This approach aligns with the recommendation of Guttman (1999) regarding the importance of distributional fit for index reliability and follows the WMO (2012) guidelines, which emphasize maintaining spatial comparability in regional drought monitoring. This choice is further supported by Stagge et al. (2015), who conducted a comprehensive evaluation of candidate probability distributions and demonstrated that the two-parameter Gamma distribution provides the most consistent fit across a wide range of climatic regimes and accumulation periods, recommending it as the standard distribution for SPI applications to ensure spatial comparability. Although alternative probability distributions and mixture models have been proposed to better represent complex precipitation regimes, their application is primarily justified in regions exhibiting strong multi-modality or heavy-tailed behavior. Preliminary exploratory analyses (not shown) did not reveal clear evidence of multi-modality in the monthly precipitation series, which is a prerequisite for the meaningful application of mixture-based distributions. In the Asi Basin, the empirical precipitation distributions were found to be reliably represented by the Gamma model, as indicated by the consistent outcomes of both goodness-of-fit tests. Under these conditions, the adoption of mixture models would increase parameter uncertainty and reduce spatial comparability without yielding a

Table 2

SPI method values and drought classification (Aksoy et al., 2021)

Drought Class	SPI Values
Mild drought	$-1.00 < SPI < 0.00$
Moderate drought	$-1.50 < SPI \leq -1.00$
Severe drought	$-2.00 < SPI \leq -1.50$
Extreme drought	$SPI \leq -2.00$

Table 3

Goodness-of-fit test results of monthly precipitation data to Gamma distribution

Station	Period	K-S Fit (Months)	A-D Fit (Months)	Decision
Antakya	1970–2021	12/12	12/12	Fit ($p > 0.05$)
Dörtyol	1970–2021	12/12	12/12	Fit ($p > 0.05$)
İskenderun	1970–2021	12/12	12/12	Fit ($p > 0.05$)
İslahiye	1970–2021	12/12	12/12	Fit ($p > 0.05$)
Samandağ	1970–2021	12/12	12/12	Fit ($p > 0.05$)
Altınözü	1987–2021	12/12	12/12	Fit ($p > 0.05$)
Arsuz-Uluçınar	1970–2021	12/12	12/12	Fit ($p > 0.05$)
Belen	1988–2021	12/12	12/12	Fit ($p > 0.05$)
Hassa	1977–2021	11/12	11/12	Fit (except Sep.)
Kırıkhan	1970–2021	11/12	11/12	Fit (except Jul.)
Yeşilkent-Erzin	1987–2021	12/12	12/12	Fit ($p > 0.05$)

statistically meaningful improvement in goodness-of-fit. Therefore, the adoption of the Gamma distribution represents a deliberate balance between statistical adequacy, parameter stability, and spatial comparability, which is essential for basin-scale drought assessments.

For all indices, seasonal values were calculated using total accumulated precipitation over the specified time scales (e.g., 3, and 12 months), rather than by aggregating or averaging monthly index values.

2.4. Percent of Normal Index (PNI)

The Percent of Normal Index, which uses only the precipitation data, is used as given in Eq. (15). Şen (2015) stated that this method is very effective under singular conditions such as a specific location or season and that the application process provides practicality in terms of analysis. Drought classification according to this method is given in Table 4.

$$PNI = \frac{P}{P_{mean}} \times 100 \tag{15}$$

Here, P is the amount of precipitation (mm) during the specified time period, P_{mean} is the average of the amount of precipitation (mm) during the specified time period.

The use of different thresholds for different accumulation periods in the Percentage of Normal Index (PNI) reflects a necessary statistical adjustment to account for the reduction in precipitation variance as the accumulation period increases. Monthly precipitation typically exhibits high variability and skewness, whereas seasonal (3–6 months) and annual (12 months) precipitation totals are progressively stabilized by temporal averaging. As a result, a given percentage deficit represents a much rarer and more hydrologically significant anomaly at longer time scales than at shorter ones. Therefore, time-scale-dependent PNI thresholds (Table 4) were adopted to ensure that drought severity classes represent comparable levels of statistical rarity and hydrological significance across monthly, seasonal, and annual

Table 4

PNI method values and drought classification

Period	Normal and above (%)	Mildly arid (%)	Moderately drought (%)	Severe drought (%)
1	> 75	65–75	55–65	< 55
3	> 75	65–75	55–65	< 55
6	> 80	70–80	60–70	< 60
9	> 83.5	73.5–83.5	63.5–73.5	< 63.5
12	> 85	75–85	65–75	< 65

Table 5

DDI method values and drought classification

Drought class	Index values
Much below normal	1–2
Below normal	3–4
Near below	5–6
Above normal	7–8
Much above normal	9–10

time scales, rather than artificially inflating short-term droughts or suppressing long-term drought detection.

2.5. Deciles Drought Index (DDI)

In order to calculate the Deciles Drought Index (DDI) values, precipitation data for each hydrological year of the relevant station are sorted from smallest to largest. This precipitation series is then divided into 10 equal parts (deciles), each representing 10% intervals. The first decile represents values not exceeding the lowest 10% of precipitation; the second decile represents values not exceeding the lowest 20%. Similarly, the third decile covers precipitation amounts that do not exceed the lowest 30% and so on up to the 10th decile. The tenth decile represents the highest precipitation in the series, while the fifth decile represents the median (Topçu & Seçkin, 2018). Drought classification according to this method is given in Table 5.

2.6. Determining the Compatibility Between Methods

The similarity ratio (SR) among the three methods was calculated based on the classification of periods as either 'drought' or 'non-drought'. As shown in Eq. (16), the overall SR was computed as the ratio of the number of periods with complete agreement to the total number of periods.

$$SR = \frac{\sum_{t=1}^{N} U_t}{N} \times 100 \qquad (16)$$

Here, SR denotes the similarity ratio, U_t represents the agreement indicator among the three drought indices, N indicates the total number of periods (depending on temporal scale), and t refers to the temporal scale (monthly, seasonal, or annual).

The value of U_t was assigned as 1 when all indices indicated the same drought condition, and 0 otherwise, as shown in Eq. (17).

$$U_t = \begin{cases} 1, & if\ R_{1,t} = R_{2.t} = R_{3,t} \\ 0, & otherwise \end{cases} \qquad (17)$$

Here, $R_{i,t}$ represents the result of method "i" at time "t" (1 = drought, 0 = non drought); i = 1,2,3 denotes the three drought identification methods. For the determination of the binary drought status ($R_{i,t}$), the drought classification thresholds presented in Tables 2, 4, and 5 were applied without recalibration. For SPI, the classification defined by Aksoy et al. (2021) was used (Table 2), where values <0 indicate drought. For PNI, time-dependent thresholds were adopted to account for the reduction in variance at longer accumulation periods (Table 4), with the "Mildly Arid" and more severe categories classified as drought. For DDI, the decile-based classification of Gibbs and Maher (1967) was applied (Table 5), where index values of 1–2 (Much below normal) and 3–4 (Below normal) were classified as drought. This framework was deliberately chosen to evaluate the consistency of the indices in their standard operational forms, ensuring that the analysis reflects practical drought-monitoring practice rather than imposing artificial statistical equivalence among fundamentally different indices.

2.7. Sensitivity Analysis Using a Common Threshold

To evaluate the robustness of the similarity analysis and to assess the influence of index-specific classification thresholds, an additional sensitivity analysis was conducted using a common drought threshold applied uniformly across all indices. In the standard approach, each drought index (SPI, PNI, and DDI) employs its own classification scheme based on different mathematical formulations and threshold definitions. While this reflects the operational use of each index, it may introduce inconsistencies in drought identification when comparing indices directly.

To address, this issue, a unified drought classification framework was introduced. In this framework, drought conditions were defined using a common percentile-based threshold derived from each index's

empirical distribution. Specifically, the driest 30th percentile of the respective time series was classified as a "drought" event equally for all three indices (SPI, PNI, and DDI). This percentile level was selected to represent a moderate drought occurrence frequency while ensuring sufficient sample size for robust comparison across time scales. This approach ensures that all indices are evaluated under statistically equivalent conditions, thereby minimizing the structural bias arising from index-specific classification schemes.

Using this common threshold, the binary drought classification (drought/non-drought) was recalculated for all time scales (monthly, seasonal, and annual), and the similarity ratio (SR) was recomputed following Eqs. (16) and (17). The resulting sensitivity-based SR values were then compared with those obtained from the original classification framework. This analysis enables the evaluation of whether the observed agreement between indices is governed primarily by their intrinsic mathematical structure or by differences in classification thresholds. Consequently, it provides a robustness check for the consistency analysis and enhances the reliability of the inter-index comparison.

The use of empirical percentiles to harmonize and objectively compare disparate drought indicators has been widely applied in comprehensive drought assessment frameworks, such as the United States Drought Monitor (USDM), which characterizes initial dry conditions at approximately the 30th percentile (Quiring, 2009; Svoboda et al., 2002). These recommendations are not intended to replace the standard formulation of the indices, but rather to enhance the comparability of their outputs under equivalent statistical conditions.

2.8. Correlation Analysis

The linear relationship between the drought indices (SPI, PNI, and DDI) was evaluated using Pearson correlation coefficients across all stations and time scales. However, hydroclimatic time series, particularly those involving overlapping accumulation periods, often exhibit temporal autocorrelation. This violates the assumption of independent observations required for classical significance testing and may lead to an overestimation of the degrees of freedom.

To provide a more robust quantification of uncertainty and to address serial dependence, 95% confidence intervals (CI) were calculated based on the effective sample size (n_{eff}). The effective sample size was estimated using a Bartlett-type correction formula based on the lag-1 autocorrelation of the compared series, as shown in Eq. (18) (Bartlett, 1946; Pyper & Peterman, 1998).

$$n_{eff} = N\frac{1-(\rho_x\rho_y)}{1+(\rho_x\rho_y)} \tag{18}$$

where N is the nominal sample size, and ρ_x and ρ_y represent the lag-1 autocorrelation coefficients of the two compared indices. The confidence intervals were then derived using Fisher's z-transformation, with the standard error adjusted according to n_{eff}.

By reporting these confidence intervals, the study provides a more realistic assessment of the reliability of the observed correlations under autocorrelated conditions. This is particularly important for interpreting the strength of agreement among the indices, such as the high DDI–PNI correlations and the comparatively more moderate SPI–DDI relationships.

2.9. Definition of Drought Events

Since each drought identification method relies on a different classification scheme, a direct comparison using a single system was not feasible. Therefore, the comparison was based solely on whether a drought event occurred, regardless of severity. A year was classified as a drought year when the annual index value was below 0 for SPI, below 5 for DDI, and below the 85th percentile for PNI. Similarly, for seasonal and monthly time scales, periods were classified as drought periods when the SPI was below 0, the DDI was below 5, and the PNI was below the 75th percentile. Values above these thresholds were classified as non-drought periods.

2.10. *Spatial analysis and Drought Mapping Procedure*

Spatial drought maps for the driest years identified by each index were generated using station-based annual drought index values (SPI-12, PNI-12, and DDI-12). The spatial distribution of drought severity across the Asi Basin was obtained using the Inverse Distance Weighting (IDW) interpolation method.

The IDW method was selected because it is a deterministic interpolation technique that assigns greater influence to nearby observations and effectively preserves local spatial variability. This characteristic is particularly important in regions with complex topography, such as the Asi Basin, where strong orographic controls (e.g., the Amanos Mountains) play a dominant role in shaping precipitation and drought patterns.

Although geostatistical methods such as ordinary kriging are widely used in spatial interpolation, the relatively sparse station network (11 stations) and strong orographic gradients in the Asi Basin may hinder reliable variogram modelling. Therefore, the deterministic IDW method was preferred in order to avoid unstable variogram estimation while preserving local spatial gradients. By constraining spatial influence based on distance, IDW also helps prevent unrealistic smoothing of drought signals across major topographic barriers (Shepard, 1968; Yüceer & Aktürk, 2025).

The IDW interpolation was performed using the formulations derived from Shepard's method (Shepard, 1968). The mathematical basis of the interpolation is expressed in Eqs. (19) and (20) as follows:

$$F(x,y) = \sum_{i=1}^{n} w_i * f_i \tag{19}$$

$$w_i = h_i^{-p} / \sum_{i=1}^{n} h_i^{-p} \tag{20}$$

Here, F(x,y) denotes the estimated drought index value at the location (x,y), f_i represents the known value at the sample point i, w_i signifies the weight assigned to each sample point (where the sum of weights equals 1), h_i indicates the spatial distance between the interpolated point and the sample point i, and p refers to the power parameter (exponent).

In IDW interpolation, the p parameter determines the influence of known points on the estimated values based on their distance; therefore, the method is sensitive to the chosen power value (Isaaks & Srivastava, 1989). Several power values were tested during the analysis. Although higher power values yielded marginally lower error statistics, they resulted in unrealistic spatial patterns by allowing the influence of stations to extend across major topographic barriers. Therefore, a power value of p = 2.5 was adopted. This value ensured that the interpolated patterns remained physically consistent with the basin's topography, specifically preventing the unrealistic propagation of precipitation signals across the Amanos Mountains.

To validate the reliability of the interpolation model, a cross-validation analysis was conducted for representative drought years. The statistical results indicated that the model produced unbiased estimates, with Mean Error (ME) values fluctuating close to zero for all indices (ranging from − 1.57 to 1.39). The Root Mean Square Error (RMSE) values were found to be within acceptable limits relative to the scale of each index: 0.52–1.02 for SPI, 11.08–12.09 for PNI, and 0.92–1.61 for DDI. These low error margins confirm that the IDW method successfully captured the spatial variability of drought in the basin. The corresponding ME and RMSE values obtained from the cross-validation analysis are summarized in Table 6. Because SPI, DDI, and PNI are expressed on different numerical scales, RMSE

Table 6

Cross-validation statistics (ME and RMSE) of IDW interpolation for the three driest years identified by each index

Drought index	Year	Mean error (ME)	RMSE
SPI-12	1989	− 0.10	1.02
	1991	0.06	0.52
	1993	− 0.06	0.56
PNI-12	1989	− 1.57	12.09
	1990	1.39	11.20
	1993	0.98	11.08
DDI-12	1989	− 0.10	1.26
	1990	0.28	0.92
	1999	0.12	1.61

values were interpreted within each index's own range and are not directly comparable across indices.

To ensure high cartographic quality, the interpolation was performed with a fine spatial resolution appropriate for basin-scale analysis. The resulting continuous raster surfaces were reclassified according to the threshold values of the SPI, PNI, and DDI indices. For visualization purposes, bilinear interpolation resampling was employed solely to smooth transitions between grid cells and reduce pixelation effects, without altering the underlying drought index values or classification thresholds. Finally, the classified drought maps were produced to visually illustrate the spatial distribution and severity of drought conditions during the selected critical years.

2.11. Mann–Kendall Trend Test

To evaluate the presence of monotonic trends in the dataset, the Mann–Kendall (M–K) trend test was applied. The M–K test is a non-parametric statistical method, originally introduced by Mann (1945) and later refined by Kendall (1975), and is widely used for detecting trends in hydro-meteorological time series.

The MK test statistic S is calculated as given in Eq. (21).

$$S = \sum_{i=1}^{n-1} \sum_{j=i+1}^{n} sgn\left(x_j - x_i\right) \tag{21}$$

where n is the number of observations, x_i and x_j denote the ith and jth observations (with $j > i$), respectively. The function $sgn(x_j - x_i)$ denotes the sign function, which is defined in Eq. (22).

$$sgn = \begin{cases} +1 & if\left(x_j - x_i\right) > 0 \\ 0 & if\left(x_j - x_i\right) = 0 \\ -1 & if\left(x_j - x_i\right) < 0 \end{cases} \tag{22}$$

The variance of S is estimated as given in Eq. (23).

$$Var(S) = \frac{n(n-1)(2n+5) - \sum_{k=1}^{m} t_k(t_k-1)(2t_k+5)}{18} \tag{23}$$

where m denotes the number of tied groups and t_k represents the number of ties in the kth group. The standardized test statistic Z is then calculated as given in Eq. (24).

$$Z = \begin{cases} \frac{S-1}{\sqrt{Var(S)}} & if\ S > 0 \\ 0 & if\ S = 0 \\ \frac{S+1}{\sqrt{Var(S)}} & if\ S < 0 \end{cases} \tag{24}$$

Here, the Z statistic is assumed to follow a standard normal distribution. The statistical significance of a trend is evaluated at a given confidence level, typically $1 - \alpha/2$. A trend is considered statistically significant if the calculated p-value is less than the significance level α(commonly 0.05 or 0.01). This is equivalent to the condition that the absolute value of Z exceeds the critical value $Z_1 - \alpha/2$. The direction of the trend is determined by the sign of the Z statistic and Kendall's τ, where positive and negative values indicate increasing and decreasing trends, respectively. It is important to emphasize that the M–K test is a non-parametric method, making it suitable for detecting trends in time series data without requiring any assumption about the underlying data distribution.

3. Result

When the monthly results of the indices were analyzed, the longest-lasting drought periods for each station were identified and are presented in Table 7. According to all three indices, an eight-month longest dry period was observed at the Antakya, İslahiye, and Altınözü stations, while a seven-month period was observed at the Yeşilkent and Erzin stations. In addition, the longest dry period was identified by the DDI and PNI indices at the Dörtyol, Samandağ, Arsuz Uluçınar, and Hassa stations. At the Belen station, the longest dry period was detected by the SPI and DDI indices.

When the monthly index values were examined over the observation period, the three methods produced generally similar drought detection results, with the exception of July and August.Analysis of the precipitation data revealed a strongly zero-dominated rainfall regime during the summer season (JJA). The proportion of zero-rainfall months varies across the basin, ranging from 4.5% at Dörtyol to 46.2% at

Table 7

The drought periods with the longest duration

Stations	Methods	The beginning of the drought	The ending of the drought	Duration (months)
Antakya	SPI-DDI-PNI	10/01/2013	05/01/2014	8
Dörtyol	SPI	09/01/1971	03/01/1972	7
		03/01/2012	09/01/2012	
		03/01/2021	09/01/2021	
	DDI	09/01/1971	02/01/1972	6
		10/01/1972	03/01/1973	
		05/01/2004	10/01/2004	
	PNI	05/01/2004	10/01/2004	6
İskenderun	SPI	09/01/1971	04/01/1972	8
		10/01/2013	05/01/2014	
	DDI	11/01/1971	04/01/1972	6
	PNI	12/01/1972	03/01/1973	4
		05/01/2003	08/01/2003	
		07/01/2007	10/01/2007	
		06/01/2011	09/01/2011	
		11/01/2013	02/01/2014	
İslahiye	SPI	09/01/2013	04/01/2014	8
	DDI–PNI	01/01/1989	08/01/1989	8
Samandağ	SPI	09/01/1971	04/01/1972	8
		10/01/2013	05/01/2014	
	DDI	03/01/1985	09/01/1985	7
		11/01/2013	05/01/2014	
	PNI	05/01/2019	11/01/2019	7
Altınözü	SPI	10/01/2013	05/01/2014	8
	DDI	01/01/1989	08/01/1989	8
		10/01/2013	05/01/2014	
	PNI	01/01/1989	08/01/1989	8
Arsuz-Uluçınar	SPI	11/01/1972	04/01/1973	6
		06/01/1977	11/01/1977	
		03/01/1985	08/01/1988	
	DDI–PNI	04/01/1989	08/01/1989	5
Belen	SPI–DDI	01/01/1989	09/01/1989	9
	PNI	04/01/1989	09/01/1989	6
Hassa	SPI	03/01/1985	09/01/1985	7
	DDI–PNI	10/01/2013	02/01/2014	5
		10/01/2016	02/01/2017	
Kırıkhan	SPI–PNI	02/01/2021	11/01/2021	10
	DDI	10/01/1972	03/01/1973	6
		05/01/1984	10/01/1984	
		02/01/2021	07/01/2021	
Yeşilkent-Erzin	SPI-DDI-PNI	01/01/1989	07/01/1989	7

İslahiye (Table 8). Even at stations with lower zero-precipitation frequencies, mean summer rainfall remains close to zero.

The linear agreement between SPI, PNI, and DDI was evaluated using Pearson correlation coefficients (r) together with 95% confidence intervals (CI) derived from Bartlett-corrected effective sample sizes (n_{eff}). The complete set of results for monthly, seasonal, and annual scales across all stations is provided in Tables 14, 15, and 16, respectively.

At the monthly scale (Table 14), the indices exhibit consistently high agreement during the wet and recharge period (November to May), with correlation coefficients generally exceeding 0.90 and accompanied by relatively narrow confidence intervals across most stations. For example, SPI–DDI correlations frequently exceed 0.95 during the wet

Table 8

Percentage of zero-precipitation months during the summer season (JJA) across the Asi Basin stations

Station (Coast → Inland)	Zero-precipitation months (%)
Antakya (inland plain)	44.2
Dörtyol (coastal)	4.5
İskenderun (coastal)	10.3
İslahiye (inland)	46.2
Samandağ (coastal)	41.0
Altınözü (inland)	31.4
Arsuz-Uluçınar (coastal)	17.9
Belen (mountain pass)	12.8
Hassa (inland)	14.7
Kırıkhan (inland)	12.8
Yeşilkent-Erzin (near-coastal)	13.5

season (November–May), with tight confidence intervals, indicating a strong and stable hydroclimatic signal across indices. However, a clear deterioration in both correlation strength and statistical certainty is observed during the dry summer months (July–August). Notably, at the Antakya station, the SPI–DDI correlation decreases to 0.657 in July, with a substantially widened confidence interval of [0.46—0.79]. Similar patterns are observed in other stations, where reduced precipitation variability and increased autocorrelation lead to a marked reduction in effective sample size, resulting in wider confidence intervals and increased uncertainty.

The seasonal results (Table 15) confirm this pattern at an aggregated temporal scale. While the DDI–PNI relationship remains consistently strong across all seasons (typically high, with r values mostly above 0.85–0.90), correlations involving SPI (SPI–DDI and SPI–PNI) show noticeable weakening during summer and winter. This seasonal divergence reflects the increased sensitivity of SPI to precipitation variability, particularly under low-precipitation and highly autocorrelated conditions.

The impact of autocorrelation becomes most pronounced at the annual scale (Table 16), where the effective sample size is substantially reduced, leading to significantly wider confidence intervals. Although DDI and PNI maintain very strong correlations across all stations ($r > 0.91$), the agreement between SPI and the other indices weakens considerably. For instance, at the Arsuz Uluçınar station, the SPI–PNI correlation is 0.311, with a confidence interval spanning -0.05 to 0.60. This indicates that the relationship is not statistically significant when accounting for autocorrelation, reflecting a reduced effective sample size. Similar widening of confidence intervals is observed at other stations, emphasizing the reduction in effective degrees of freedom at longer temporal scales.

Overall, the inclusion of Bartlett-corrected confidence intervals provides a more transparent and statistically realistic assessment of inter-index agreement. The results demonstrate that the apparent consistency between drought indices is strongly influenced not only by their conceptual formulation but also by the effective information content of the time series and the underlying hydroclimatic conditions of the Asi Basin.

Initial assessments based on original classification schemes indicated that inter-index agreement is highly dependent on temporal scale. Notably, December exhibited the highest agreement, reaching up to 100% similarity at the Antakya station (Table 9), while seasonal results generally showed greater similarity than annual index results (Table 10).

To further investigate these patterns, a sensitivity analysis based on a common percentile threshold was conducted, providing important insight into the influence of classification schemes on the similarity ratio (SR) results. The harmonized approach revealed that the effect of threshold definitions on inter-index agreement is not uniform across stations and time scales. As shown in Tables 9, 10, 11, and 12, the SR values obtained using the common 30th percentile threshold exhibit both increases and decreases relative to the original classification framework, indicating that the impact of threshold asymmetry is context-dependent.

At the monthly scale, the discrepancies observed during the dry summer months were partially reduced at some stations, while in others the agreement decreased, reflecting the sensitivity of the indices to threshold selection under zero-precipitation conditions. In particular, months characterized by extremely low or zero precipitation show variable responses to threshold harmonization across stations. Similarly, the very high agreement values observed

Table 9

Similarity rates (%) of the three methods in detecting drought based only on monthly index results

Stations	Months											
	Jan	Feb	Mar	Apr	May	Jun	Jul	Aug	Sep	Oct	Nov	Dec
Antakya	78.85	80.77	82.69	80.77	92.31	88.46	21.15	23.08	90.38	100.00	96.15	92.31
Dörtyol	84.62	86.54	86.54	92.31	98.08	88.46	84.62	88.46	96.15	82.69	92.31	96.15
İskenderun	84.62	84.62	73.08	76.92	94.23	90.38	86.54	88.46	96.15	71.15	78.85	92.31
İslahiye	73.08	94.23	90.38	82.69	84.62	84.62	25.00	17.31	88.46	84.62	98.08	94.23
Samandağ	92.31	94.23	80.77	78.85	96.15	92.31	25.00	25.00	90.38	90.38	88.46	94.23
Altınözü	74.29	88.57	82.86	91.43	74.29	94.29	28.57	17.14	88.57	97.14	80.00	88.57
Arsuz-Uluçınar	71.88	81.25	71.88	90.63	84.38	84.38	84.38	100.00	90.63	78.13	65.63	90.63
Belen	82.35	91.18	73.53	85.29	91.18	85.29	88.24	85.29	97.06	85.29	88.24	97.06
Hassa	82.22	88.89	84.44	91.11	84.44	84.44	95.56	88.89	66.67	91.11	97.78	93.33
Kırıkhan	75.00	69.23	75.00	88.46	80.77	92.31	50.00	88.46	88.46	92.31	90.38	88.46
Yeşilkent-Erzin	80.00	94.29	82.86	91.43	71.43	82.86	91.43	91.43	88.57	94.29	94.29	88.57

Table 10

Similarity rates (%) of the three methods in detecting drought based only on seasonal and annual index results

Stations	Spring	Summer	Autumn	Winter	Annual
Antakya	82.69	71.15	73.08	88.46	60.78
Dörtyol	76.92	80.77	88.46	65.38	50.98
İskenderun	69.23	71.15	67.31	65.38	60.78
İslahiye	84.62	73.08	84.62	71.15	47.06
Samandağ	76.92	80.77	69.23	86.54	64.71
Altınözü	74.29	62.86	91.43	68.57	58.82
Arsuz-Uluçınar	68.75	84.38	50.00	84.38	64.52
Belen	76.47	88.24	88.24	79.41	57.58
Hassa	80.00	84.44	71.11	80.00	56.82
Kırıkhan	82.69	86.54	65.38	86.54	64.71
Yeşilkent-Erzin	80.00	88.57	82.86	68.57	55.88

Table 11

Similarity rates (%) of the three methods in detecting drought using a common 30th percentile threshold at the monthly scale

Stations	Months											
	Jan	Feb	Mar	Apr	May	Jun	Jul	Aug	Sep	Oct	Nov	Dec
Antakya	69.23	80.77	71.15	82.69	94.23	86.54	26.92	36.54	88.46	88.46	90.38	86.54
Dörtyol	88.46	80.77	80.77	86.54	88.46	94.23	90.38	92.31	96.15	84.62	86.54	86.54
İskenderun	86.54	82.69	82.69	80.77	88.46	90.38	92.31	96.15	86.54	84.62	78.85	88.46
İslahiye	65.38	88.46	78.85	84.62	88.46	86.54	32.69	21.15	88.46	88.46	86.54	73.08
Samandağ	80.77	78.85	75.00	63.46	90.38	88.46	28.85	30.77	88.46	90.38	90.38	86.54
Altınözü	62.86	85.71	80.00	82.86	80.00	94.29	34.29	20.00	91.43	97.14	77.14	82.86
Arsuz-Uluçınar	78.12	96.88	84.38	100.0	93.75	87.50	96.88	53.12	84.38	90.62	93.75	93.75
Belen	82.35	79.41	70.59	82.35	82.35	91.18	97.06	91.18	97.06	85.29	79.41	94.12
Hassa	84.44	80.00	84.44	91.11	86.67	100.0	97.78	57.78	88.89	93.33	93.33	86.67
Kırıkhan	84.62	78.85	84.62	84.62	90.38	94.23	50.00	94.23	92.31	88.46	88.46	88.46
Yeşilkent-Erzin	85.71	82.86	82.86	85.71	82.86	94.29	82.86	82.86	88.57	88.57	85.71	74.29

Table 12

Similarity rates (%) of the three methods in detecting drought using a common 30th percentile threshold at seasonal and annual scales

Stations	Spring	Summer	Autumn	Winter	Annual
Antakya	76.92	78.85	78.85	73.08	74.51
Dörtyol	67.31	78.85	78.85	67.31	56.86
İskenderun	69.23	76.92	78.85	65.38	76.47
İslahiye	78.85	65.38	86.54	63.46	54.90
Samandağ	76.92	84.62	67.31	76.92	70.59
Altınözü	65.71	74.29	94.29	57.14	64.71
Arsuz-Uluçınar	68.75	71.88	71.88	78.12	56.25
Belen	67.65	73.53	85.29	70.59	69.70
Hassa	77.78	80.00	84.44	71.11	61.36
Kırıkhan	69.23	73.08	76.92	75.00	68.63
Yeşilkent-Erzin	74.29	74.29	77.14	77.14	64.71

during wetter winter months under the original classification were moderated under the unified threshold, resulting in a more balanced representation of inter-index consistency.

A direct comparison between the original results (Tables 9 and 10) and the sensitivity analysis (Tables 11 and 12) shows that threshold harmonization generally improves agreement at the annual scale (e.g., from 60.78% to 74.51% at Antakya), while notable differences between indices persist at finer temporal scales, particularly at the monthly level.

The seasonal and annual analyses further confirm that threshold harmonization does not lead to a systematic increase in similarity ratios, but rather modifies the magnitude and variability of agreement depending on climatic conditions and temporal aggregation. While improvements in SR values are observed at some stations and time scales, decreases are also evident in others, highlighting the complex interaction between index formulation and classification criteria.

Overall, these findings demonstrate that differences in drought classification thresholds contribute to variations in SR values, and that both the intrinsic characteristics of the indices and the selected classification schemes jointly control the observed agreement patterns. Consequently, the sensitivity analysis confirms that inter-index consistency is influenced not only by methodological differences but also by the definition of drought thresholds, particularly under extreme climatic conditions.

The spatial distribution maps of drought severity were generated using the IDW method for the identified driest years. The analysis of these maps reveals that drought characteristics were not spatially uniform but exhibited distinct local variations across the basin. The spatial patterns of drought for all three indices are collectively presented in Fig. 2. In this figure, the maps are organized by index, with SPI-12 in the top row, PNI-12 in the middle row, and DDI-12 in the bottom row, displaying the chronologically ordered driest years for each method. A comparison of the spatial patterns in Fig. 2 indicates that 1989 was the most critical year, consistently identified as a widespread drought period by all three indices. In that year, drought conditions appear to be spatially widespread across the basin; however, this spatial interpretation should be considered in relation to the limited station density used for interpolation. As shown in the top row (SPI-12), Extreme Drought conditions dominated the northern sub-basins (e.g., Hassa and İslahiye). Similarly, the bottom row (DDI-12) characterizes 1989 as a uniformly severe drought year, with the entire basin classified as Much Below Normal. In contrast, for the other identified drought years (e.g., 1991 for SPI or 1990 for PNI), drought severity exhibited a more heterogeneous spatial structure, with intensified conditions confined primarily to specific sub-regions rather than affecting the basin as a whole.

The results of the Mann–Kendall (M–K) trend analysis for the annual SPI, PNI, and DDI across the 11 meteorological stations are presented in Table 13. Overall, most stations did not exhibit statistically significant trends ($p > 0.05$) during the study period. However, a statistically significant decreasing trend

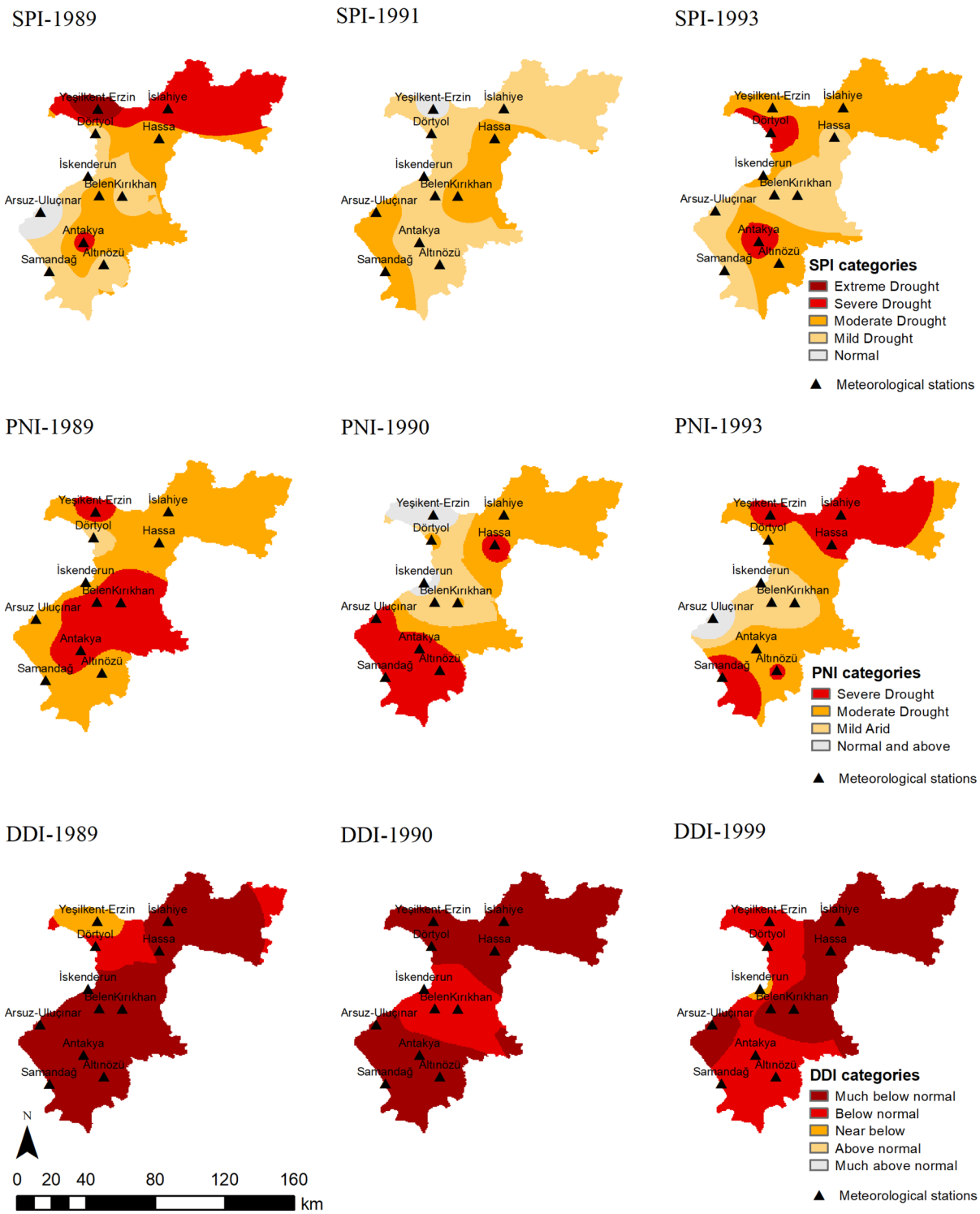


Figure 2

Spatial distribution of drought severity for the selected dry years identified by SPI-12 (top row), PNI-12 (middle row), and DDI-12 (bottom row) using the IDW interpolation method. Meteorological station locations are indicated by black triangles to provide a clear reference for the primary data sources. The interpolated surfaces illustrate indicative spatial patterns of drought conditions and should be interpreted in relation to the available meteorological station network rather than as exact spatial boundaries of drought severity

Table 13

Mann–Kendall trend analysis results for annual SPI, PNI, and DDI at the meteorological stations

Stations	Index	Kendall's Tau (τ)	p-value
Antakya	SPI	− 0.004	0.9741
Antakya	DDI	0.024	0.8179
Antakya	PNI	0.029	0.7799
Dörtyol	SPI	0.005	0.9611
Dörtyol	DDI	0.061	0.5410
Dörtyol	PNI	0.086	0.3880
İskenderun	SPI	0.119	0.2200
İskenderun	DDI	0.166	0.0955
İskenderun	PNI	0.169	0.0856
İslahiye	SPI	0.021	0.8327
İslahiye	DDI	0.035	0.7328
İslahiye	PNI	0.026	0.7963
Samandağ	SPI	0.042	0.6728
Samandağ	DDI	0.058	0.5623
Samandağ	PNI	0.021	0.8407
Altınözü	SPI	− 0.080	0.5142
Altınözü	DDI	− 0.171	0.1657
Altınözü	PNI	− 0.148	0.2339
Arsuz-Uluçınar	SPI	− 0.054	0.6833
Arsuz-Uluçınar	DDI	0.029	0.8320
Arsuz-Uluçınar	PNI	0.056	0.6765
Belen	SPI	0.000	1.0000
Belen	DDI	− 0.102	0.4205
Belen	PNI	− 0.113	0.3754
Hassa	SPI	− 0.224	0.0328
Hassa	DDI	− 0.276	0.0102
Hassa	PNI	− 0.295	0.0062
Kırıkhan	SPI	− 0.082	0.3983
Kırıkhan	DDI	− 0.043	0.6740
Kırıkhan	PNI	− 0.052	0.6056
Yeşilkent-Erzin	SPI	0.045	0.7220
Yeşilkent-Erzin	DDI	− 0.038	0.7641
Yeşilkent-Erzin	PNI	− 0.033	0.7964

was consistently identified at the Hassa station for all three indices, with Kendall's τ values of − 0.224 ($p = 0.033$) for SPI, − 0.276 ($p = 0.010$) for DDI, and − 0.295 ($p = 0.006$) for PNI. In contrast, the remaining stations, including Antakya, Dörtyol, and İslahiye, showed near-zero τ values and non-significant p-values, indicating the absence of a clear monotonic trend in these locations.

4. Discussion

The analysis of the monthly results revealed a strong agreement among the three drought indices (SPI, PNI, and DDI) at several stations—particularly Antakya, İslahiye, and Altınözü—indicating a high degree of methodological consistency in drought detection. The simultaneous identification of prolonged monthly drought periods by all indices suggests that these areas are hydrologically more sensitive to precipitation deficits and exhibit a persistent drought signal. In contrast, at stations such as Dörtyol, Samandağ, Arsuz Uluçınar, Hassa, and Belen, where agreement was observed between only two indices, the discrepancies likely reflect differences in the temporal response and sensitivity of each index to monthly precipitation variability. These spatial inconsistencies highlight the complementary nature of the indices and emphasize the importance of adopting a multi-index framework for a more comprehensive characterization of drought conditions across the basin.

The reduced agreement among the indices during the summer months can be attributed to the Mediterranean climate regime, which is characterized by very dry summers. Under such conditions, minimal precipitation limits the sensitivity of precipitation-based indices, leading to lower agreement between methods. The observed divergence between drought indices during summer is primarily driven by the zero-dominated rainfall regime identified in the Results section rather than by computational or statistical artifacts. Under these conditions (4.5–46.2% zero-precipitation frequency), the Percentage of Normal Index (PNI) becomes mathematically unstable because the long-term mean precipitation in the denominator approaches zero, such that even small rainfall amounts (e.g., 5–10 mm) produce disproportionately large anomaly values. In contrast, the SPI, computed using the WMO standard software (WMO, 2012), incorporates the probability of zero precipitation (q) into the cumulative distribution function H(x), thereby maintaining probabilistic stability under extremely dry summer conditions. Conversely, the high agreement observed in December reflects the more stable and precipitation-rich winter conditions. Furthermore, the greater similarity at the seasonal scale compared to the annual scale indicates that drought detection consistency improves at finer temporal resolutions. This suggests that monthly and seasonal analyses capture the temporal dynamics of precipitation variability more effectively than annual assessments.

The results further demonstrate that the observed reduction in inter-index agreement during dry periods is accompanied by a substantial increase in statistical uncertainty. The Bartlett-corrected confidence intervals reveal that, particularly during summer and at longer temporal scales, the effective sample size is significantly reduced due to strong temporal autocorrelation. As a consequence, even moderate correlation coefficients may not represent statistically robust relationships. This is especially evident at the annual scale, where several SPI-based correlations exhibit wide confidence intervals, in some cases spanning values close to zero. These findings indicate that the apparent weakening of agreement between indices is not solely a function of their differing formulations but is also strongly influenced by the reduced effective degrees of freedom in autocorrelated hydroclimatic time series.

The stronger agreement observed between the DDI and PNI methods at seasonal and annual scales suggests that these indices share a similar response to precipitation variability, likely due to their comparable algebraic formulations based on direct precipitation ratios. In contrast, the SPI exhibits weaker correlations with these indices under dry summer conditions. This divergence is expected because SPI standardizes precipitation anomalies into a normalized probabilistic distribution, whereas PNI and DDI remain sensitive to the absolute magnitude of rainfall deficits. Consequently, the 'mathematical hypersensitivity' of PNI in arid months (as discussed above) weakens its correlation with the probabilistically robust SPI. To address the mathematical instability of the PNI during zero-dominated summer months, specific operational adjustments are recommended for drought monitoring in the Asi Basin and similar Mediterranean climates. It is advisable to interpret the PNI with caution or consider limiting its use in assessments during peak summer months (particularly July and August), especially at inland stations where the long-term mean monthly precipitation falls below a critical threshold (e.g., < 10 mm) or where the frequency of zero-precipitation months is exceptionally high. Under these hyper-arid conditions, minor absolute variations in precipitation can result in mathematically disproportionate and physically misleading anomaly percentages. Instead, for operational drought monitoring and early warning systems, probabilistic indices such as the SPI may be more appropriate, as they explicitly integrate the probability of zero precipitation into their cumulative distribution functions, thereby mitigating the risk of false drought or anomalous wetness alarms. If the use of algebraic indices is necessary for continuity, applying a minimum precipitation threshold before calculating the PNI is suggested to mask out months where the climatological mean is too low to produce stable ratios. These recommendations are not intended to replace the standard formulation of the PNI, but rather to enhance its interpretability under climatological conditions where its underlying assumptions are violated. This behavior is consistent

with previous findings; Vicente-Serrano et al. (2012) reported weaker correlations between SPI and other precipitation-based indices during summer conditions in the Northern Hemisphere, highlighting the effect of dry-season variability on inter-index consistency.

The results of this study provide a comprehensive evaluation of the consistency between SPI, PNI, and DDI across multiple temporal scales in the Asi Basin. Overall, the three indices exhibited a generally consistent ability to detect drought conditions, particularly during periods characterized by sufficient precipitation. High similarity ratios and strong correlations observed during the wetter months and seasons indicate that all three indices capture the dominant hydroclimatic signal under normal and wet conditions. However, a marked divergence between the indices was observed during the dry summer months, especially in July and August. This period is characterized by a zero-dominated precipitation regime, where a substantial proportion of observations consists of zero rainfall values. Under such conditions, the fundamental assumptions underlying precipitation-based drought indices are challenged. While probabilistic indices such as the SPI are specifically designed to accommodate zero precipitation within their distributional framework, algebraic indices such as the PNI and, to a lesser extent, the DDI may exhibit amplified variability. As a result, even minor absolute differences in precipitation can lead to disproportionately large changes in index values, contributing to reduced inter-index agreement during summer. The instability of the PNI under low-precipitation conditions is particularly evident in inland stations such as İslahiye, where the frequency of zero-precipitation months is high. In these environments, the ratio-based formulation of the PNI becomes highly sensitive to small variations in precipitation, which may result in misleading drought classifications. Therefore, caution should be exercised when interpreting PNI values during dry periods, and its use may be complemented or, if necessary, limited during zero-dominated conditions.

To further investigate whether these discrepancies arise from methodological differences or classification-related effects, an additional sensitivity analysis was performed. The sensitivity analysis conducted using a common percentile-based threshold revealed that the influence of classification schemes on similarity ratio (SR) results is not uniform across stations and time scales. While the harmonized framework reduced discrepancies at some stations and time periods, it also led to decreased agreement in others, indicating that the effect of threshold selection is context-dependent. These findings demonstrate that part of the observed discrepancies between indices is attributable to differences in classification thresholds. However, the persistence of differences even under the unified framework demonstrates that intrinsic differences in index formulation also play a significant role in shaping inter-index agreement. This is further supported by the notable increase in annual agreement observed at stations such as Antakya under the unified threshold, suggesting that while threshold harmonization improves consistency at longer time scales, discrepancies at shorter temporal scales are more strongly governed by the intrinsic mathematical responses of the indices to extreme dryness.

These findings highlight that drought assessment outcomes are not solely determined by the choice of index but are also influenced by both classification strategies and the underlying climatic characteristics of the study region. In Mediterranean-type climates such as the Asi Basin, where precipitation is highly seasonal and summer rainfall is nearly absent, the interpretation of drought indices requires careful consideration of both methodological and climatological constraints. Finally, the spatial analysis results should be interpreted in light of the limitations associated with station density and interpolation methodology. The use of the IDW method, combined with a relatively sparse meteorological network, may not fully capture localized orographic precipitation gradients, particularly in regions influenced by the Amanos Mountains. Therefore, the spatial patterns presented in this study should be considered as indicative representations of drought conditions rather than precise delineations of drought severity. Overall, the results demonstrate that while SPI, PNI, and DDI provide broadly consistent drought signals under most conditions, their agreement is strongly modulated by both climatic characteristics and methodological choices. These findings underscore the importance of using multiple indices and carefully selected classification frameworks when

conducting drought assessments in complex climatic regions.

Similarly, Vergni et al. (2021) showed that in Mediterranean regions, agreement decreases during the spring–summer period due to the positively skewed rainfall distribution and the Gamma-based standardization used in SPI. Furthermore, Nohegar et al. (2015) noted differences in drought identification between PNI/DDI and SPI in southern Iran, supporting the conclusion that precipitation-based indices (PNI/DDI) and probabilistic indices (SPI) provide complementary information in arid and semi-arid regions. Although all three indices are derived from the same precipitation records, they apply fundamentally different mathematical transformations (probabilistic, algebraic, and rank-based). If the observed agreement were merely due to mathematical co-variation, consistency would be uniform across all seasons and stations. Instead, the strong winter agreement and reduced summer agreement, together with the systematic differences between SPI and the algebraic indices (PNI and DDI), demonstrate that the results reflect physically meaningful drought-signal behavior rather than trivial statistical dependence.

The concurrence observed for 1989 indicates that this year represents a basin-wide drought event of substantial magnitude, likely associated with large-scale precipitation deficits affecting southern Türkiye. Spatial drought maps generated for this year reveal a largely homogeneous drought pattern across the Asi Basin, with high drought severity extending over nearly the entire region for all three indices. This consistency suggests that 1989 corresponds to a synoptic-scale drought event, in which large-scale atmospheric circulation anomalies dominated local controls. In contrast, the simultaneous identification of 1990 by the DDI and PNI reflects the strong agreement between these two precipitation-based indices, which directly represent cumulative rainfall anomalies without relying on probabilistic standardization. Similarly, the detection of 1993 by both SPI and PNI suggests that these indices are particularly sensitive to intense but relatively short-term precipitation deficits. By comparison, the years 1991 and 1999, which were identified by only a single index, likely correspond to more localized or less persistent drought episodes, for which methodological sensitivity and temporal aggregation become decisive. While 1989 represented a relatively homogeneous drought event, other drought years exhibited pronounced spatial heterogeneity. This variability can be largely attributed to the strong orographic influence of the Amanos Mountains, which intercept moisture-laden air masses from the Mediterranean and generate sharp precipitation gradients across the basin. As a result, drought impacts in years such as 1991 and 1999 remained spatially localized rather than propagating uniformly across the basin. The IDW interpolation with a power parameter of $p = 2.5$ effectively captured these local variations by constraining spatial influence with distance, thereby preventing unrealistic drought signal propagation across major topographic barriers. However, it is crucial to acknowledge the limitations inherent in the spatial interpolation of precipitation-based indices over complex terrain using a relatively sparse network of 11 stations. While the IDW method provides a valuable macro-scale visualization of drought patterns, it cannot capture the exact micro-scale orographic precipitation gradients across the Amanos Mountains with absolute precision. Furthermore, as reflected by the cross-validation RMSE values (e.g., 11.08–12.09 for PNI), the resulting continuous raster surfaces should be interpreted as qualitative, indicative spatial patterns rather than reliable quantitative representations of local drought severity. At the same time, it is important to note that, despite these limitations, the interpolation approach remains suitable for identifying basin-scale spatial patterns and relative drought variability. The primary objective of this study is not to provide precise point-scale estimations, but rather to reveal the spatial consistency and comparative behavior of drought indices across the basin. To overcome these limitations and enhance the spatial resolution of regional drought monitoring, establishing a denser meteorological observation network across the basin is highly recommended as a future priority.

Overall, the stronger agreement observed between DDI and PNI compared to SPI—particularly for multi-year drought conditions—can be attributed to their shared reliance on direct precipitation anomalies rather than standardized probabilistic transformations. This distinction highlights the complementary

nature of algebraic and probabilistic drought indices in capturing drought processes operating at different temporal and spatial scales. Furthermore, the spatial drought maps generated in this study demonstrate that reliance on a single index may overlook localized drought events or underestimate cumulative precipitation deficits. Therefore, effective drought monitoring and water resource management strategies in the Asi Basin should adopt a multi-index framework that accounts for both the statistical characteristics of different drought indices and the strong sub-regional topographic controls identified in this study.

The absence of a basin-wide statistically significant trend suggests that drought evolution in the Asi Basin is spatially heterogeneous, reflecting the high climatic variability of the Eastern Mediterranean region. However, the consistent and statistically significant decreasing trends observed at the Hassa station across all three indices are particularly noteworthy.

This agreement among SPI, PNI, and DDI indicates that the detected drought signal is robust and not sensitive to the methodological differences between indices. Although not statistically significant ($p > 0.05$), the negative Kendall's τ values observed in stations such as Altınözü and Kırıkhan may indicate a tendency toward drier conditions in the inner parts of the basin. These findings are consistent with the results reported by Topçu and Seçkin (2022), who identified an increase in drought frequency in the Asi Basin after the 1990s. In contrast, the absence of significant trends in coastal stations such as İskenderun may be attributed to maritime influences, which can moderate regional drying signals.

5. Conclusions

This study evaluated drought conditions in the Asi Basin at monthly, seasonal, and annual time scales using three precipitation-based indices (SPI, DDI, and PNI) and long-term precipitation records from 11 meteorological stations. The consistency among these indices was assessed to determine their reliability in representing drought dynamics under Mediterranean climate conditions. This study applied the Mann–Kendall test to assess temporal trends in SPI, PNI, and DDI across the Asi Basin. While no basin-wide significant trend was detected, a consistent decreasing trend was identified at the Hassa station across all indices. These results highlight the spatial heterogeneity of drought dynamics and emphasize the importance of localized assessments for water management and climate adaptation in the region.

- At the monthly scale, the three drought indices showed strong agreement at key stations, particularly Antakya, İslahiye, and Altınözü, indicating a consistent detection of drought conditions across hydrologically sensitive areas of the Asi Basin. The highest overall consistency was observed during winter months, especially in December, when precipitation patterns are more stable.
- Discrepancies during the summer months highlight the mathematical instability of the PNI under zero-dominated rainfall regimes. Consequently, for operational drought monitoring in the Asi Basin, it is recommended to interpret the PNI with caution or apply a minimum precipitation threshold during peak summer months (July–August). During these hyper-arid periods, probabilistically robust indices like the SPI are generally preferred to avoid false alarms.
- Inter-index consistency was higher at monthly and seasonal time scales than at the annual scale, indicating that shorter temporal resolutions better capture drought dynamics. This supports the use of high-resolution drought monitoring for early warning and adaptive water management in the Asi Basin, with DDI and PNI providing particularly consistent and practical tools for operational applications.
- This study shows that the agreement between SPI, PNI, and DDI varies with temporal scale and climatic conditions in the Asi Basin, with stronger consistency at monthly and seasonal scales but reduced agreement during dry summer periods and at the annual scale. The use of Bartlett-corrected confidence intervals demonstrates that temporal autocorrelation reduces the effective sample size and increases uncertainty, indicating that some moderate correlations may not be statistically robust. Overall, the complementary behavior of

SPI, PNI, and DDI highlights the importance of a multi-index framework that accounts for both climatic variability and statistical uncertainty in drought assessment.

- The sensitivity analysis using a common percentile-based threshold demonstrated that part of the observed differences between drought indices arises from variations in classification schemes rather than solely from their intrinsic mathematical structure. The results indicate that threshold harmonization alters similarity ratios across stations and time scales rather than producing a uniform increase, highlighting the combined influence of methodological design and threshold selection on drought assessment outcomes.
- The consistent identification of 1989 by all three indices indicates a basin-wide drought, while partial agreement in other years highlights the value of a multi-index approach for distinguishing spatially heterogeneous drought events.
- Water managers in the Asi Basin may benefit from combining SPI for monitoring long-term moisture deficits (which can serve as a proxy for potential hydrological drought) with DDI and PNI for seasonal agricultural drought monitoring to support more robust decision-making.
- The complementary behavior of SPI, PNI, and DDI highlights the importance of a multi-index approach for robust drought assessment in the Asi Basin. Future studies should incorporate additional climatic variables, such as temperature and evapotranspiration, to further improve drought characterization in Mediterranean-type regions.

Author Contributions All authors contributed to the study conception and design. Material preparation, data collection and analysis were performed by Mehmet Can Topboğazı, Seda Sever and Recep Yurtal. The first draft of the manuscript was written by Seda Sever and all authors commented on previous versions of the manuscript. All authors read and approved the final manuscript.

Funding

Open access funding provided by the Scientific and Technological Research Council of Türkiye (TÜBİTAK).

Data Availability

On reasonable request, data supporting the fndingsof this study can be obtained from the Turkish State Meteorological Service (https://www.mgm.gov.tr/).

Declarations

Conflict of interest The authors have no relevant financial or non-financial interests to disclose.

Ethical approval Not applicable.

Consent to participate Not applicable.

Consent to publication Not applicable.

Open Access This article is licensed under a Creative Commons Attribution 4.0 International License, which permits use, sharing, adaptation, distribution and reproduction in any medium or format, as long as you give appropriate credit to the original author(s) and the source, provide a link to the Creative Commons licence, and indicate if changes were made. The images or other third party material in this article are included in the article's Creative Commons licence, unless indicated otherwise in a credit line to the material. If material is not included in the article's Creative Commons licence and your intended use is not permitted by statutory regulation or exceeds the permitted use, you will need to obtain permission directly from the copyright holder. To view a copy of this licence, visit http://creativecommons.org/licenses/by/4.0/.

Appendix 1: Supplementary tables of correlation coefficients and confidence intervals

See Tables 14, 15, and 16.

Table 14

Monthly Pearson correlation coefficients (r) and 95% confidence intervals (CI) computed using Bartlett-corrected effective sample sizes (n_{eff}) for the selected meteorological stations

Months	Methods	Antakya	Dörtyol	İskenderun	İslahiye
Jan	SPI-DDI (r [CI])	0.982 [0.97- 0.99]	0.985 [0.97–0.99]	0.981 [0.97–0.99]	0.973 [0.95–0.98]
	SPI-PNI (r [CI])	0.904 [0.84–0.94]	0.896 [0.82–0.94]	0.921 [0.86–0.95]	0.896 [0.83–0.94]
	DDI-PNI (r [CI])	0.911 [0.85–0.95]	0.920 [0.86–0.95]	0.911 [0.85–0.95]	0.887 [0.81–0.93]
Feb	SPI-DDI (r [CI])	0.831 [0.72–0.90]	0.902 [0.83–0.94]	0.925 [0.87–0.96]	0.927 [0.87–0.96]
	SPI-PNI (r [CI])	0.895 [0.83–0.94]	0.934 [0.89–0.96]	0.935[0.89–0.96]	0.953 [0.92–0.97]
	DDI-PNI (r [CI])	0.871 [0.79–0.93]	0.912 [0.85–0.95]	0.913 [0.85–0.95]	0.894 [0.82–0.94]
Mar	SPI-DDI (r [CI])	0.958 [0.93–0.98]	0.940 [0.90–0.97]	0.981 [0.97–0.99]	0.954 [0.92–0.97]
	SPI-PNI (r [CI])	0.894 [0.82–0.94]	0.957 [0.93–0.97]	0.905 [0.84–0.94]	0.915 [0.86–0.95]
	DDI-PNI (r [CI])	0.915 [0.86–0.95]	0.924 [0.87–0.96]	0.903 [0.84–0.94]	0.906 [0.84–0.95]
Apr	SPI-DDI (r [CI])	0.963 [0.94–0.98]	0.962 [0.93–0.98]	0.926 [0.87–0.96]	0.955 [0.92–0.97]
	SPI-PNI (r [CI])	0.882 [0.80–0.93]	0.940 [0.90–0.97]	0.933 [0.88–0.96]	0.913 [0.85–0.95]
	DDI-PNI (r [CI])	0.897 [0.83–0.94]	0.917 [0.86–0.95]	0.875 [0.79–0.93]	0.897 [0.83–0.94]
May	SPI-DDI (r [CI])	0.958 [0.93–0.98]	0.955 [0.92–0.97]	0.965 [0.94–0.98]	0.962 [0.93–0.98]
	SPI-PNI (r [CI])	0.866 [0.77–0.92]	0.934 [0.89–0.96]	0.912 [0.85–0.95]	0.906 [0.84–0.95]
	DDI-PNI (r [CI])	0.918 [0.86–0.95]	0.922 [0.87–0.95]	0.925 [0.87–0.96]	0.898 [0.83–0.94]
Jun	SPI-DDI (r [CI])	0.949 [0.91–0.97]	0.987 [0.98–0.99]	0.990 [0.98–0.99]	0.949 [0.91–0.97]
	SPI-PNI (r [CI])	0.815 [0.69–0.89]	0.916[0.86–0.95]	0.932 [0.88–0.96]	0.818 [0.70–0.89]
	DDI-PNI (r [CI])	0.912 [0.84–0.95]	0.904 [0.84–0.94]	0.922 [0.87–0.96]	0.930 [0.88–0.96]
Jul	SPI-DDI (r [CI])	0.657 [0.46–0.79]	0.983 [0.97–0.99]	0.936 [0.89–0.96]	0.808 [0.67–0.89]
	SPI-PNI (r [CI])	0.728 [0.57–0.84]	0.875 [0.79–0.93]	0.801 [0.68–0.88]	0.860 [0.75–0.92]
	DDI-PNI (r [CI])	0.899 [0.83–0.94]	0.911 [0.85–0.95]	0.927 [0.88–0.96]	0.940 [0.90–0.97]
Aug	SPI-DDI (r [CI])	0.766 [0.62–0.86]	0.987 [0.98–0.99]	0.987 [0.98–0.99]	0.777 [0.64–0.87]
	SPI-PNI (r [CI])	0.832 [0.72–0.90]	0.917 [0.86–0.95]	0.889 [0.81–0.94]	0.896 [0.82–0.94]
	DDI-PNI (r [CI])	0.931 [0.88–0.96]	0.921 [0.86–0.95]	0.920 [0.86–0.95]	0.857 [0.76–0.92]
Sep	SPI-DDI (r [CI])	0.963 [0.94–0.98]	0.976 [0.96–0.99]	0.942 [0.90–0.97]	0.845 [0.74–0.91]
	SPI-PNI (r [CI])	0.844 [0.74–0.91]	0.913 [0.85–0.95]	0.900 [0.83–0.94]	0.717 [0.56–0.83]
	DDI-PNI (r [CI])	0.922 [0.87–0.95]	0.924 [0.87–0.96]	0.919 [0.86–0.95]	0.920 [0.86–0.95]
Oct	SPI-DDI (r [CI])	0.964 [0.94–0.98]	0.955 [0.92–0.97]	0.983 [0.97–0.99]	0.944 [0.90–0.97]
	SPI-PNI (r [CI])	0.937 [0.89–0.96]	0.920 [0.86–0.95]	0.879 [0.80–0.93]	0.900 [0.83–0.94]
	DDI-PNI (r [CI])	0.927 [0.87–0.96]	0.896 [0.82–0.94]	0.898 [0.83–0.94]	0.903 [0.83–0.94]
Nov	SPI-DDI (r [CI])	0.967 [0.94–0.98]	0.962 [0.93–0.98]	0.942 [0.90–0.97]	0.957 [0.93–0.97]
	SPI-PNI (r [CI])	0.943 [0.90–0.97]	0.921 [0.87–0.95]	0.893 [0.82–0.94]	0.941 [0.90–0.97]
	DDI-PNI (r [CI])	0.923 [0.87–0.96]	0.903 [0.84–0.94]	0.862 [0.77–0.92]	0.911 [0.85–0.95]
Dec	SPI-DDI (r [CI])	0.879 [0.80–0.93]	0.931 [0.88–0.96]	0.873 [0.78–0.93]	0.920 [0.86–0.95]
	SPI-PNI (r [CI])	0.916 [0.86–0.95]	0.928 [0.87–0.96]	0.914 [0.85–0.95]	0.915 [0.85–0.95]
	DDI-PNI (r [CI])	0.924 [0.87–0.96]	0.923 [0.86–0.96]	0.926 [0.87–0.96]	0.909 [0.84–0.95]
Months	Methods	Samandağ	Altınözü	Arsuz-Uluçınar	Belen
Jan	SPI-DDI (r [CI])	0.987 [0.98–0.99]	0.965 [0.93–0.98]	0.979 [0.96–0.99]	0.981 [0.96–0.99]
	SPI-PNI (r [CI])	0.947 [0.91–0.97]	0.891 [0.79–0.94]	0.890 [0.78–0.95]	0.910 [0.82–0.95]
	DDI-PNI (r [CI])	0.931 [0.88–0.96]	0.903 [0.81–0.95]	0.902 [0.80–0.95]	0.916 [0.84–0.96]
Feb	SPI-DDI (r [CI])	0.868 [0.78–0.92]	0.876 [0.76–0.94]	0.970 [0.94–0.99]	0.832 [0.68–0.92]
	SPI-PNI (r [CI])	0.921 [0.86–0.95]	0.946 [0.89–0.97]	0.913 [0.83–0.96]	0.923 [0.85–0.96]
	DDI-PNI (r [CI])	0.909 [0.84–0.95]	0.902 [0.81–0.95]	0.887 [0.78–0.94]	0.917 [0.84–0.96]
Mar	SPI-DDI (r [CI])	0.969 [0.94–0.98]	0.940 [0.88–0.97]	0.968 [0.93–0.98]	0.955 [0.91–0.98]
	SPI-PNI (r [CI])	0.891 [0.81–0.94]	0.911 [0.83–0.95]	0.841 [0.69–0.92]	0.895 [0.80–0.95]
	DDI-PNI (r [CI])	0.902 [0.83–0.94]	0.881 [0.77–0.94]	0.922 [0.83–0.96]	0.880 [0.77–0.94]
Apr	SPI-DDI (r [CI])	0.928 [0.88–0.96]	0.982 [0.96–0.99]	0.923 [0.85–0.96]	0.865 [0.73–0.93]
	SPI-PNI (r [CI])	0.812 [0.69–0.89]	0.929 [0.85–0.97]	0.904 [0.81–0.95]	0.941 [0.88–0.97]
	DDI-PNI (r [CI])	0.905 [0.84–0.94]	0.898 [0.79–0.95]	0.909 [0.82–0.96]	0.863 [0.72–0.94]
May	SPI-DDI (r [CI])	0.973 [0.95–0.98]	0.937 [0.88–0.97]	0.959 [0.91–0.98]	0.929 [0.86–0.97]
	SPI-PNI (r [CI])	0.883 [0.80–0.93]	0.820 [0.66–0.91]	0.807 [0.62–0.91]	0.906 [0.81–0.95]
	DDI-PNI (r [CI])	0.914 [0.85–0.95]	0.880 [0.77–0.94]	0.915 [0.82–0.96]	0.886 [0.77–0.94]

Table 14 *continued*

Months	Methods	Samandağ	Altınözü	Arsuz-Uluçınar	Belen
Jun	SPI-DDI (r [CI])	0.957 [0.93–0.98]	0.925 [0.85–0.96]	0.932 [0.86–0.97]	0.980 [0.96–0.99]
	SPI-PNI (r [CI])	0.865 [0.78–0.92]	0.799 [0.63–0.90]	0.796 [0.62–0.90]	0.859 [0.73–0.93]
	DDI-PNI (r [CI])	0.912 [0.85–0.95]	0.909 [0.82–0.95]	0.916 [0.83–0.96]	0.908 [0.82–0.95]
Jul	SPI-DDI (r [CI])	0.810 [0.69–0.89]	0.841 [0.68–0.92]	0.941 [0.88–0.97]	0.931 [0.86–0.97]
	SPI-PNI (r [CI])	0.904 [0.84–0.94]	0.900 [0.79–0.95]	0.763 [0.56–0.88]	0.791 [0.62–0.89]
	DDI-PNI (r [CI])	0.890 [0.82–0.94]	0.941 [0.87–0.97]	0.914 [0.83–0.96]	0.935 [0.87–0.97]
Aug	SPI-DDI (r [CI])	0.795 [0.67–0.88]	0.669 [0.43–0.82]	0.816 [0.66–0.91]	0.898 [0.80–0.95]
	SPI-PNI (r [CI])	0.871 [0.78–0.92]	0.820 [0.67–0.91]	0.646 [0.39–0.81]	0.760 [0.56–0.88]
	DDI-PNI (r [CI])	0.878 [0.80–0.93]	0.836 [0.70–0.91]	0.959 [0.91–0.98]	0.932 [0.86–0.97]
Sep	SPI-DDI (r [CI])	0.987 [0.98–0.99]	0.962 [0.93–0.98]	0.976 [0.95–0.99]	0.965 [0.93–0.98]
	SPI-PNI (r [CI])	0.918 [0.86–0.95]	0.834 [0.69–0.91]	0.882 [0.77–0.94]	0.901 [0.81–0.95]
	DDI-PNI (r [CI])	0.922 [0.87–0.96]	0.903 [0.81–0.95]	0.919 [0.84–0.96]	0.915 [0.84–0.96]
Oct	SPI-DDI (r [CI])	0.958 [0.93–0.98]	0.972 [0.94–0.99]	0.967 [0.93–0.98]	0.920 [0.84–0.96]
	SPI-PNI (r [CI])	0.922 [0.87–0.96]	0.956[0.91–0.98]	0.856 [0.73–0.93]	0.895 [0.80–0.95]
	DDI-PNI (r [CI])	0.911 [0.85–0.95]	0.926 [0.85–0.96]	0.911 [0.82–0.96]	0.908 [0.82–0.95]
Nov	SPI-DDI (r [CI])	0.969 [0.95–0.98]	0.958 [0.92–0.98]	0.932 [0.86–0.97]	0.947 [0.89–0.97]
	SPI-PNI (r [CI])	0.934 [0.89–0.96]	0.910 [0.83–0.95]	0.887 [0.78–0.94]	0.916 [0.84–0.96]
	DDI-PNI (r [CI])	0.895 [0.82–0.94]	0.870 [0.76–0.93]	0.850 [0.71–0.92]	0.868 [0.75–0.93]
Dec	SPI-DDI (r [CI])	0.900 [0.83–0.94]	0.977 [0.95–0.99]	0.938 [0.87–0.97]	0.970 [0.93–0.99]
	SPI-PNI (r [CI])	0.900 [0.83–0.94]	0.940 [0.88–0.97]	0.945 [0.89–0.97]	0.951 [0.89–0.98]
	DDI-PNI (r [CI])	0.907 [0.84–0.95]	0.924 [0.85–0.96]	0.916 [0.83–0.96]	0.922 [0.82–0.97]

Months	Methods	Hassa	Kırıkhan	Yeşilkent-Erzin
Jan	SPI-DDI (r [CI])	0.970 [0.95–0.98]	0.976 [0.96–0.99]	0.978 [0.96–0.99]
	SPI-PNI (r [CI])	0.926 [0.87–0.96]	0.883 [0.81–0.93]	0.904 [0.82–0.95]
	DDI-PNI (r [CI])	0.909 [0.84–0.95]	0.913 [0.85–0.95]	0.923 [0.85–0.96]
Feb	SPI-DDI (r [CI])	0.952 [0.91–0.97]	0.963 [0.94–0.98]	0.918 [0.84–0.96]
	SPI-PNI (r [CI])	0.942 [0.90–0.97]	0.888 [0.81–0.93]	0.958 [0.92–0.98]
	DDI-PNI (r [CI])	0.892 [0.81–0.94]	0.849 [0.75–0.91]	0.902 [0.81–0.95]
Mar	SPI-DDI (r [CI])	0.963 [0.93–0.98]	0.961 [0.93–0.98]	0.976 [0.95–0.99]
	SPI-PNI (r [CI])	0.916 [0.85–0.95]	0.891 [0.81–0.94]	0.922 [0.85–0.96]
	DDI-PNI (r [CI])	0.890 [0.81–0.94]	0.893 [0.82–0.94]	0.914 [0.83–0.96]
Apr	SPI-DDI (r [CI])	0.922 [0.86–0.96]	0.938 [0.89–0.96]	0.936 [0.87–0.97]
	SPI-PNI (r [CI])	0.891 [0.81–0.94]	0.910 [0.85–0.95]	0.956 [0.91–0.98]
	DDI-PNI (r [CI])	0.909 [0.84–0.95]	0.894 [0.82–0.94]	0.867 [0.74–0.93]
May	SPI-DDI (r [CI])	0.966 [0.94–0.98]	0.971 [0.95–0.98]	0.969 [0.94–0.98]
	SPI-PNI (r [CI])	0.904 [0.83–0.95]	0.879 [0.80–0.93]	0.874 [0.76–0.94]
	DDI-PNI (r [CI])	0.884 [0.79–0.94]	0.898 [0.83–0.94]	0.921 [0.85–0.96]
Jun	SPI-DDI (r [CI])	0.954 [0.92–0.97]	0.965 [0.94–0.98]	0.975 [0.95–0.99]
	SPI-PNI (r [CI])	0.797 [0.65–0.89]	0.852 [0.75–0.91]	0.874 [0.75–0.94]
	DDI-PNI (r [CI])	0.911 [0.84–0.95]	0.921 [0.86–0.95]	0.927 [0.85–0.97]
Jul	SPI-DDI (r [CI])	0.982 [0.97–0.99]	0.803 [0.67–0.89]	0.899 [0.81–0.95]
	SPI-PNI (r [CI])	0.899 [0.82–0.94]	0.587 [0.36–0.75]	0.786 [0.61–0.89]
	DDI-PNI (r [CI])	0.907 [0.84–0.95]	0.736 [0.56–0.85]	0.925 [0.85–0.96]
Aug	SPI-DDI (r [CI])	0.846 [0.73–0.91]	0.941 [0.90–0.97]	0.935 [0.87–0.97]
	SPI-PNI (r [CI])	0.692 [0.50–0.82]	0.807 [0.68–0.89]	0.869 [0.75–0.93]
	DDI-PNI (r [CI])	0.948 [0.91–0.97]	0.918 [0.86–0.95]	0.919 [0.84–0.96]
Sep	SPI-DDI (r [CI])	0.857 [0.75–0.92]	0.937 [0.89–0.96]	0.956 [0.91–0.98]
	SPI-PNI (r [CI])	0.684 [0.48–0.82]	0.804 [0.68–0.88]	0.854 [0.73–0.92]
	DDI-PNI (r [CI])	0.873 [0.78–0.93]	0.912 [0.85–0.95]	0.905 [0.82–0.95]
Oct	SPI-DDI (r [CI])	0.971 [0.95–0.98]	0.939 [0.89–0.97]	0.964 [0.93–0.98]
	SPI-PNI (r [CI])	0.880 [0.79–0.93]	0.921 [0.86–0.96]	0.956 [0.91–0.98]
	DDI-PNI (r [CI])	0.929 [0.87–0.96]	0.912 [0.85–0.95]	0.927 [0.86–0.96]
Nov	SPI-DDI (r [CI])	0.916 [0.85–0.95]	0.956 [0.92–0.97]	0.924 [0.85–0.96]
	SPI-PNI (r [CI])	0.916 [0.85–0.95]	0.947 [0.91–0.97]	0.929 [0.86–0.96]
	DDI-PNI (r [CI])	0.911 [0.84–0.95]	0.909 [0.84–0.95]	0.895 [0.80–0.95]

Table 14 *continued*

Months	Methods	Hassa	Kırıkhan	Yeşilkent-Erzin
Dec	SPI-DDI (r [CI])	0.961 [0.93–0.98]	0.933 [0.88–0.96]	0.954 [0.89–0.98]
	SPI-PNI (r [CI])	0.915 [0.85–0.95]	0.941 [0.90–0.97]	0.927 [0.83–0.97]
	DDI-PNI (r [CI])	0.908 [0.84–0.95]	0.890 [0.81–0.94]	0.913 [0.78–0.97]

Table 15

Seasonal Pearson correlation coefficients (r) and 95% confidence intervals (CI) computed using Bartlett-corrected effective sample sizes (n_{eff}) for the selected meteorological stations

Seasons	Methods	Antakya	Dörtyol	İskenderun	İslahiye
Spring	SPI-DDI (r [CI])	0.846 [0.74–0.91]	0.778 [0.64–0.87]	0.670 [0.48–0.80]	0.874 [0.79–0.93]
	SPI-PNI (r [CI])	0.796 [0.67–0.88]	0.723 [0.56–0.83]	0.665 [0.47–0.80]	0.805 [0.68–0.88]
	DDI-PNI (r [CI])	0.923 [0.87–0.96]	0.923 [0.87–0.96]	0.943 [0.90–0.97]	0.920 [0.86–0.95]
Summer	SPI-DDI (r [CI])	0.721 [0.55–0.83]	0.899 [0.83–0.94]	0.754 [0.61–0.85]	0.799 [0.67–0.88]
	SPI-PNI (r [CI])	0.651 [0.45–0.79]	0.834 [0.73–0.90]	0.693 [0.52–0.81]	0.666 [0.48–0.80]
	DDI-PNI (r [CI])	0.925 [0.87–0.96]	0.884 [0.80–0.93]	0.900 [0.83–0.94]	0.928 [0.88–0.96]
Autumn	SPI-DDI (r [CI])	0.933 [0.89–0.96]	0.890 [0.82–0.94]	0.871 [0.78–0.92]	0.929 [0.88–0.96]
	SPI-PNI (r [CI])	0.842 [0.74–0.91]	0.842 [0.74–0.91]	0.822 [0.71–0.90]	0.892 [0.82–0.94]
	DDI-PNI (r [CI])	0.919 [0.86–0.95]	0.936 [0.89–0.96]	0.928 [0.88–0.96]	0.931 [0.88–0.96]
Winter	SPI-DDI (r [CI])	0.780 [0.64–0.87]	0.760 [0.61–0.86]	0.765 [0.62–0.86]	0.853 [0.76–0.91]
	SPI-PNI (r [CI])	0.670 [0.48–0.80]	0.645 [0.45–0.78]	0.659 [0.47–0.79]	0.740 [0.59–0.84]
	DDI-PNI (r [CI])	0.925 [0.87–0.96]	0.884 [0.80–0.93]	0.873 [0.79–0.93]	0.914 [0.85–0.95]
Seasons	Methods	Samandağ	Altınözü	Arsuz-Uluçınar	Belen
Spring	SPI-DDI (r [CI])	0.807 [0.68–0.88]	0.744 [0.55–0.86]	0.719 [0.47–0.86]	0.655 [0.41–0.81]
	SPI-PNI (r [CI])	0.772 [0.63–0.86]	0.664 [0.43–0.82]	0.622 [0.32–0.81]	0.669 [0.42–0.82]
	DDI-PNI (r [CI])	0.928 [0.88–0.96]	0.909 [0.83–0.95]	0.911 [0.82–0.96]	0.911 [0.83–0.95]
Summer	SPI-DDI (r [CI])	0.797 [0.66–0.88]	0.621 [0.37–0.79]	0.721 [0.50–0.85]	0.647 [0.32–0.84]
	SPI-PNI (r [CI])	0.753 [0.60–0.85]	0.606 [0.35–0.78]	0.697 [0.46–0.84]	0.612 [0.27–0.82]
	DDI-PNI (r [CI])	0.912 [0.85–0.95]	0.918 [0.84–0.96]	0.922 [0.85–0.96]	0.908 [0.80–0.96]
Autumn	SPI-DDI (r [CI])	0.863 [0.77–0.92]	0.917 [0.82–0.96]	0.714 [0.49–0.85]	0.784 [0.61–0.89]
	SPI-PNI (r [CI])	0.733 [0.57–0.84]	0.900 [0.80–0.95]	0.680 [0.43–0.83]	0.798 [0.63–0.89]
	DDI-PNI (r [CI])	0.889 [0.81–0.94]	0.931 [0.85–0.97]	0.946 [0.89–0.97]	0.911 [0.83–0.95]
Winter	SPI-DDI (r [CI])	0.837 [0.73–0.90]	0.638 [0.39–0.80]	0.771 [0.58–0.88]	0.598 [0.32–0.78]
	SPI-PNI (r [CI])	0.758 [0.61–0.85]	0.571 [0.30–0.76]	0.739 [0.52–0.87]	0.602 [0.33–0.78]
	DDI-PNI (r [CI])	0.911 [0.85–0.95]	0.942 [0.89–0.97]	0.909 [0.82–0.96]	0.914 [0.82–0.96]
Seasons	Methods	Hassa	Kırıkhan	Yeşilkent-Erzin	
Spring	SPI-DDI (r [CI])	0.873 [0.78–0.93]	0.828 [0.72–0.90]	0.766 [0.58–0.88]	
	SPI-PNI (r [CI])	0.809 [0.68–0.89]	0.782 [0.65–0.87]	0.715 [0.50–0.85]	
	DDI-PNI (r [CI])	0.900 [0.82–0.94]	0.929 [0.88–0.96]	0.900 [0.81–0.95]	
Summer	SPI-DDI (r [CI])	0.737 [0.56–0.85]	0.766 [0.62–0.86]	0.808 [0.64–0.90]	
	SPI-PNI (r [CI])	0.664 [0.46–0.80]	0.673 [0.49–0.80]	0.801 [0.63–0.90]	
	DDI-PNI (r [CI])	0.921 [0.86–0.96]	0.929 [0.88–0.96]	0.928 [0.86–0.96]	
Autumn	SPI-DDI (r [CI])	0.910 [0.84–0.95]	0.899 [0.83–0.94]	0.839 [0.70–0.92]	
	SPI-PNI (r [CI])	0.853 [0.75–0.92]	0.862 [0.77–0.92]	0.774 [0.59–0.88]	
	DDI-PNI (r [CI])	0.924 [0.86–0.96]	0.908 [0.84–0.95]	0.916 [0.84–0.96]	
Winter	SPI-DDI (r [CI])	0.844 [0.73–0.91]	0.813 [0.69–0.89]	0.772 [0.57–0.89]	
	SPI-PNI (r [CI])	0.769 [0.61–0.87]	0.731 [0.57–0.84]	0.690 [0.45–0.84]	
	DDI-PNI (r [CI])	0.919 [0.86–0.96]	0.925 [0.87–0.96]	0.923 [0.85–0.96]	

Table 16

Pearson correlation coefficients (r) and 95% confidence intervals (CI) computed using Bartlett-corrected effective sample sizes (n_{eff})

Stations	SPI-DDI (r [CI])	SPI-PNI (r [CI])	DDI-PNI (r [CI])
Antakya	0.695 [0.51–0.81]	0.665 [0.48–0.80]	0.911 [0.85–0.95]
Dörtyol	0.533 [0.30–0.71]	0.455 [0.20–0.65]	0.946 [0.91–0.97]
İskenderun	0.625 [0.42–0.77]	0.631 [0.43–0.77]	0.942 [0.89–0.97]
İslahiye	0.488 [0.25–0.67]	0.400 [0.14–0.61]	0.926 [0.87–0.96]
Samandağ	0.621 [0.41–0.77]	0.525 [0.29–0.70]	0.932 [0.88–0.96]
Altınözü	0.546 [0.25–0.75]	0.497 [0.19–0.72]	0.938 [0.89–0.97]
Arsuz-Uluçınar	0.420 [0.07–0.67]	0.311 [-0.05–0.60]	0.932 [0.86–0.97]
Belen	0.417 [0.08–0.66]	0.430 [0.10–0.67]	0.927 [0.86–0.97]
Hassa	0.538 [0.28–0.72]	0.477 [0.19–0.68]	0.947 [0.90–0.97]
Kırıkhan	0.658 [0.46–0.76]	0.601 [0.39–0.75]	0.957 [0.92–0.98]
Yeşilkent-Erzin	0.683 [0.44–0.83]	0.671 [0.43–0.82]	0.938 [0.88–0.97]

Publisher's Note Springer Nature remains neutral with regard to jurisdictional claims in published maps and institutional affiliations.

References

Abramowitz, M., & Stegun, I. A. (1965). *Handbook of mathematical formulas, graphs and mathematical tables*. Dover Publications Inc.

Aksoy, H., Çetin, M., Eriş, E., et al. (2021). Critical drought intensity-duration-frequency curves based on total probability theorem-coupled frequency analysis. *Hydrological Sciences Journal, 66*(8), 1337–1358. https://doi.org/10.1080/02626667.2021.1934473

Arra, A. E., & Sisman, E. (2024). A comprehensive analysis and comparison of SPI and SPEI for spatiotemporal drought evaluation. *Environmental Monitoring and Assessment, 196*, 980. https://doi.org/10.1007/s10661-024-13127-7

Bartlett, M. S. (1946). On the Theoretical specification and sampling properties of autocorrelated time-series. *Supplement to the Journal of the Royal Statistical Society, 8*(1), 27–41. https://doi.org/10.2307/2983611

Çelik, M. A. (2019). Akdeniz kıyılarında ekstrem nemli ve kurak mevsimlerin dağılımı (1967–2016). *Academic Platform Journal of Engineering and Science, 7*(1), 56–66.

Çetin, M., Aksoy, H., Önöz, B., et al. (2018) Deriving accumulated precipitation deficits from drought severity-duration-frequency surves: a case study in Adana province, Turkey. In *1st International congress on agricultural structures and irrigation* (pp 39–48). Antalya, Turkey.

Degefu, M. A., & Bewket, W. (2015). Trends and spatial patterns of drought incidence in the omo-ghibe river basin, ethiopia. *Geografiska Annaler: Series a, Physical Geography, 97*(2), 395–414. https://doi.org/10.1111/geoa.12080

Dikici, M. (2019). Drought analysis in the Asi Basin (Turkey). *Journal of Natural Hazards and Environment, 5*(1), 22–40. https://doi.org/10.21324/dacd.426784

Dikici, M. (2020). Drought analysis with different indices for the Asi Basin (Turkey). *Scientific Reports, 10*, 20739. https://doi.org/10.1038/s41598-020-77827-z

Dikici, M., & Aksel, M. (2021). Comparison of drought indices in the case of the Ceyhan Basin. *International Journal of Environment and Geoinformatics, 8*(2), 113–125. https://doi.org/10.30897/ijegeo.792379

Dogan, S., Berktay, A., & Singh, V. P. (2012). Comparison of multi-monthly rainfall-based drought severity indices, with application to semi-arid Konya closed basin, Turkey. *Journal of Hydrology*. https://doi.org/10.1016/j.jhydrol.2012.09.003

Gibbs, W. J., & Maher, J. V. (1967). *Rainfall deciles as drought indicators*. Bureau of Meteorology Bulletin, 48.

Gümüş, V. (2017). hydrological drought analysis of Asi River Basin with streamflow drought index. *Gazi University Journal of Science Part C: Design and Technology, 5*(1), 65–73.

Guttman, N. B. (1999). Accepting the standardized precipitation index: A calculation algorithm. *Journal of the American Water Resources Association, 35*(2), 311–322.

Hao, Z., Hao, F., Singh, V. P., Xia, Y., Ouyang, W., & Shen, X. (2016). A theoretical drought classification method for the multivariate drought index based on distribution properties of standardized drought indices. *Advances in Water Resources, 92*, 240–247. https://doi.org/10.1016/j.advwatres.2016.04.010

Heim, R. R. (2002). A Review of twentieth-century drought indices used in the United States. *Bulletin of the American Meteorological Society, 83*(8), 1–12. https://doi.org/10.1175/1520-0477-83.8.1149

IPCC. (2021). Summary for policymakers. In Masson-Delmotte, V., Zhai, P., Pirani, A., Connors, S. L., Péan, C., Berger, S., Caud, N., Chen, Y., Goldfarb, L., Gomis, M. I., Huang, M., Leitzell, K., Lonnoy, E., Matthews, J. B. R., Maycock, T. K., Waterfield, T., Yelekçi, O., Yu, R., & Zhou, B. (Eds), *Climate change 2021: the physical science basis. Contribution of Working Group I to the sixth assessment report of the intergovernmental panel on climate change* (**in press**).

IPCC. (2023). Sections. In: *Climate change 2023: synthesis report. Contribution of Working Groups I, II and III to the sixth assessment report of the intergovernmental panel on climate change [Core Writing Team, H. Lee and J. Romero (eds.)]*. IPCC, Geneva, Switzerland (pp. 35–115). https://doi.org/10.59327/IPCC/AR6-9789291691647

Jain, V. K., Pandey, R. P., Jain, M. K., & Byun, H. R. (2015). Comparison of drought indices for appraisal of drought characteristics in the Ken River Basin. *Weather and Climate Extremes, 8*, 1–11. https://doi.org/10.1016/j.wace.2015.05.002

Kendall, M. G. (1975). *Rank correlation methods* (4th ed.). London.

Keskiner, A. D., Cetin, M., Simsek, M., Akin, S., & Cetiner, I. (2019). Drought analysis with Standardized Precipitation Index and Normal Precipitation Index methods in geographic information systems environment: A case study in Seyhan Basin. *Fresenius Environmental Bulletin (FEB), 28*(7), 5675–5688.

Keyantash, J., & Dracup, J. A. (2002). The quantification of drought: An evaluation of drought Indices. *Bulletin of the American Meteorological Society, 83*(8), 1167–1180. https://doi.org/10.1175/1520-0477-83.8.1167

Labudová, L., Labuda, M., & Takáč, J. (2017). Comparison of SPI and SPEI applicability for drought impact assessment on crop production in the Danubian Lowlandand the East Slovakian Lowland. *Theoretical and Applied Climatology, 128*, 491–506. https://doi.org/10.1007/s00704-016-1870-2

Li, J., Li, Y., Yin, L., & Zhao, Q. (2024). A novel composite drought index combining precipitation, temperature and evapotranspiration used for drought monitoring in the Huang-Huai-Hai Plain. *Agricultural Water Management, 291*, Article 108626. https://doi.org/10.1016/j.agwat.2023.108626

Lloyd-Hughes, B., & Saunders, M. A. (2002). A drought climatology for Europe. *International Journal of Climatology, 22*(13), 1571–1592. https://doi.org/10.1002/joc.846

Mann, H. B. (1945). Non-parametric test against trend. *Econometrica, 13*, 245–259.

Mckee, T. B., Doesken, N. J., & Kleist, J. (1993). The relatıonship of drought frequency and duration to time scales. In *Eighth conference on applied climatology* (pp. 17–22).

Mishra, A. K., & Singh, V. P. (2010). A review of drought concepts. *Journal of Hydrology, 391*(1), 202–216. https://doi.org/10.1016/j.jhydrol.2010.07.012

Morid, S., Smakhtin, V., & Moghaddasi, M. (2006). Comparison of seven meteorologıcal indices for drought monıtorıng in Iran. *International Journal of Climatology, 26*, 971–985. https://doi.org/10.1002/joc.1264

Nikbakht, J., Tabari, H., & Talaee, P. H. (2013). Streamflow drought severity analysis by percent of normal index (PNI) in northwest Iran. *Theoretical and Applied Climatology, 112*(3–4), 565–573. https://doi.org/10.1007/s00704-012-0750-7

Nohegar, A., Mahmoodabadi, S., & Norouzi, A. (2015). Comparison the suitability of SPI, PNI and DI drought index in Kahurestan Watershed (Hormozgan Province/South of Iran). *Journal of Environment and Earth Science, 5*(8), 71–76.

Öz, F. Y., Özelkan, E., & Tatlı, H. (2024). Comparative analysis of SPI, SPEI, and RDI indices for assessing spatio-temporal variation of drought in Turkey. *Earth Science Informatics, 17*(5), 4473–4505. https://doi.org/10.1007/s12145-024-01401-8

Özfidaner, M. (2020). *Precipitation and streamflow drought index to drought analysis scale of Turkey and determination to be drought probability*. PhD thesis, Çukurova University.

Palmer, W. (1965). *Meteorological drought.* Research Paper 45. Washington.

Pyper, B. J., & Peterman, R. M. (1998). Comparison of methods to account for autocorrelation in correlation analyses of fish data. *Canadian Journal of Fisheries and Aquatic Sciences, 55*, 2127–2140.

Quiring, S. M. (2009). Monitoring Drought: An Evaluation of Meteorological Drought Indices. *Geography Compass, 3*, 64–88. https://doi.org/10.1111/j.1749-8198.2008.00207.x

Salehnia, N., Alizadeh, A., Sanaeinnejad, H., Bannayan, M., Zarrin, A., & Hoogenboom, G. (2017). Estimation of meteorological drought indices based on AgMERRA precipitation data and station-observed precipitation data. *Journal of Arid Land, 9*(6), 797–809. https://doi.org/10.1007/s40333-017-0070-y

Şen, Z. (2015). *Applied drought modeling, prediction, and mitigation*. Elsevier.

Serkendiz, H., Tatli, H., Kılıç, A., Çetin, M., & Sungur, A. (2024). Analysis of drought intensity, frequency and trends using the spei in Turkey. *Theoretical and Applied Climatology, 155*(4), 2997–3012. https://doi.org/10.1007/s00704-023-04772-y

Shepard, D. (1968). A two-dimensional interpolation function for irregularly-spaced data. In *Proceedings of the 1968 23rd ACM national conference,* pp. 517–524. https://doi.org/10.1145/800186.810616

Shokoohi, A., & Morovati, R. (2015). Basinwide comparison of RDI and SPI within an IWRM framework. *Water Resources Management, 29*, 2011–2026. https://doi.org/10.1007/s11269-015-0925-y

Şimşek, O. (2010). *Drought evaluation of agricultural year and drought-yield analysis of wheat by crop growth model in Turkey*. PhD thesis, Ankara University.

Şimsek, O., & Çakmak, B. (2010). Drought analysis for 2007–2008 agricultural year of Turkey. *Journal of Tekirdag Agricultural Faculty, 7*(3), 99–109.

Soláková, T., Michele, C. D., & Vezzoli, R. (2014). Comparison between parametric and nonparametric approaches for the calculation of two drought indices: SPI and SSI. *Journal of Hydrologic Engineering, 19*, 9. https://doi.org/10.1061/(ASCE)HE.1943-5584.0000942

Stagge, J. H., Tallaksen, L. M., Gudmundsson, L., Loon, A. F. V., & Stahl, K. (2015). Candidate distributions for climatological drought indices (SPI and SPEI). *International Journal of Climatology, 35*(13), 4027–4040. https://doi.org/10.1002/joc.4267

Svoboda, M., et al. (2002). The drought monitor. *Bulletin of the American Meteorological Society, 83*(8), 1181–1190.

Thom, H. C. S. (1958). A note on the gamma distribution. *Monthly Weather Review, 86*, 117–122. https://doi.org/10.1175/1520-0493(1958)086%3c0117:ANOTGD%3e2.0.CO;2

Tirivarombo, S., Osupile, D., & Eliasson, P. (2018). Drought monitoring and analysis: standardised precipitation evapotranspiration index (SPEI) and standardised precipitation index (SPI). *Physics and Chemistry of the Earth, Parts a/b/c, 106*, 1–10. https://doi.org/10.1016/j.pce.2018.07.001

Topboğazı, M. C., Sever, S., Çetin, M., & Yurtal, R. (2022). Drought assessment for some selected stations in the orontes river basin by Standardized Precipitation Index. *11. Ulusal Hidroloji Kongresi*, Gaziantep, Turkey, pp. 325–332.

Topçu, E., & Seçkin, N. (2018). Drought analysis of East Mediterranean, Seyhan, Ceyhan and Asi Basins by using various methods. In *3rd International Mediterranean science and engineering congress (IMSEC),* Adana, Turkey, 2018.

Topçu, E., & Seçkin, N. (2022). Drought assessment using the reconnaissance drought index (RDI): A case study of Eastern Mediterranean, Seyhan, Ceyhan, and Asi basins of Turkey. *Journal of Engineering Research (Kuwait), 10*(2), 124–141. https://doi.org/10.36904/jer.12113

Topçu, E., Seçkin, N., & Haktanır, N. A. (2022). Drought analyses of Eastern Mediterranean, Seyhan, Ceyhan, and Asi Basins by using aggregate drought index (ADI). *Theoretical and Applied Climatology, 147*(3), 909–924. https://doi.org/10.1007/s00704-021-03873-w

Turhan, E., Çulha, B. D., & Değerli, S. (2022). Hydrological evaluation of streamflow drought ındex method for different time scales: A case study of Arsuz Plain, Turkey. *Journal of Natural Hazards and Environment, 8*(1), 25–36. https://doi.org/10.21324/dacd.903655

Vergni, L., Todisco, F., & Lena, B. D. (2021). Evaluation of the similarity between drought indices by correlation analysis and Cohen's Kappa test in a Mediterranean area. *Natural Hazards, 108*, 2187–2209. https://doi.org/10.1007/s11069-021-04775-w

Vicente-Serrano, S. M., Beguería, S., & López-Moreno, S. I. (2010). A multiscalar drought index sensitive to global warming: The Standardized Precipitation Evapotranspiration Index. *Journal of Climate, 23*(7), 1696–1718. https://doi.org/10.1175/2009JCLI2909.1

Vicente-Serrano, S. M., Beguería, S., Lorenzo-Lacruz, J., Camarero, J. J., López-Moreno, J. I., Azorin-Molina, C., Revuelto, J., Morán-Tejeda, E., & Sanchez-Lorenzo, A. (2012). Performance of drought indices for ecological, agricultural, and hydrological applications. *Earth Interactions, 16*(10), 1–27. https://doi.org/10.1175/2012EI000434.1

Vicente-Serrano, S. M., López-Moreno, J. L., Beguería, S., Lorenzo-Lacruz, J., Azorin-Molina, C., & Morán-Tejeda, E. (2011). Accurate computation of a streamflow drought Index. *Journal of Hydrologic Engineering, 17*(2), 318–332. https://doi.org/10.1061/(ASCE)HE.1943-5584.0000433

Wable, P. S., Jha, M. K., & Shekhar, A. (2018). Comparison of drought indices in a semi-arid river basin of India. *Water Resources Management, 33*, 75–102. https://doi.org/10.1007/s11269-018-2089-z

Wilhite, D. A., & Glantz, M. H. (1985). Understanding: The drought phenomenon: The role of definitions. *Water International, 10*(3), 111–120. https://doi.org/10.1080/02508068508686328

WMO. (2012). *Standardized precipitation index user guide*. Geneva.

WMO. (2022). *Drought and water scarcity*. Geneva.

World Meteorological Organization (WMO), & Global Water Partnership (GWP). (2016). *Handbook of drought indicators and indices (M. Svoboda and B.A. Fuchs)*. Integrated Drought Management Programme (IDMP), Integrated Drought Management Tools and Guidelines Series 2. Geneva.

Wu, H., Hayes, M. J., Weiss, A., & Hu, Q. (2001). An evaluation of the standardized precipitation index, the China-Z Index and the Statistical S-Score. *International Journal of Climatology, 21*, 745–758. https://doi.org/10.1002/joc.658

Yihdego, Y., Vaheddoost, B., & Al-Weshah, R. A. (2019). Drought indices and indicators revisited. *Arabian Journal of Geosciences, 12*(3), 1–12. https://doi.org/10.1007/s12517-019-4237-z

Yüceer, D., & Aktürk, G. (2025). Spatio-temporal characteristics of meteorological droughts using RDI and SPI in the Kizilirmak Basin of Türkiye. *Pure and Applied Geophysics*. https://doi.org/10.1007/s00024-025-03826-8

Zeybekoğlu, U., & Aktürk, G. (2021). A comparison of the China-Z Index (CZI) and the Standardized Precipitation Index (SPI) for drought assessment in the Hirfanli Dam basin in central Turkey. *Arabian Journal of Geosciences, 14*, 2731. https://doi.org/10.1007/s12517-021-09095-8

Zhai, J., Su, B., Krysanova, V., Vetter, T., Gao, C., & Jiang, T. (2010). Spatial variation and trends in PDSI and SPI indices and their relation to streamflow in 10 large regions of China. *Jounal of Climate, 23*(3), 649–663. https://doi.org/10.1175/2009JCLI2968.1

(Received October 17, 2025, revised April 13, 2026, accepted May 6, 2026)